Novel polyvinyl chloride ultrafiltration membranes blended with amphiphilic polyethylene glycol-block-poly(1, 2-dichloroethylene) copolymer for oily wastewater treatment

M. Monsefi Khosroshahi[1], Y. Jafarzadeh[1,*], M. Nasiri[2], M. Khayet[3,4,*]

[1] Faculty of Chemical Engineering, Sahand University of Technology, Tabriz, Iran.

[2] Faculty of Polymer Engineering, Sahand University of Technology, Tabriz, Iran.

[3] Department of Structure of Matter, Thermal Physics and Electronics, Faculty of Physics, University Complutense of Madrid, Avda. Complutense s/n, 28040, Madrid, Spain.

[4] Madrid Institute for Advanced Studies of Water (IMDEA Water Institute), Calle Punto Net Nº 4, 28805, Alcalá de Henares, Madrid, Spain.

* Corresponding authors:

khayetm@fis.ucm.es (M. Khayet)

yjafarzadeh@sut.ac.ir (Y. Jafarzadeh)

Abstract

Amphiphilic di-block copolymer consisting of polyethylene glycol (PEG) and poly(1,2-dichloroethylene) (PDCE) blocks was synthesized following the atom transfer radical polymerization (ATRP) procedure. The chemical structure of the obtained di-block copolymer PEG-b-PDCE was confirmed by different characterization techniques. Polyvinyl chloride (PVC) blend PEG-b-PDCE ultrafiltration (UF) membranes (PVC/PEG-b-PDCE) were prepared using the non-solvent induced phase separation (NIPs) technique and their characteristics were investigated as a function of the PEG-b-PDCE blending ratio in the casting solution. Water contact angle, permeate flux, and oil–water emulsion separation tests were performed to evaluate the hydrophilic character, permeability and anti-fouling membrane performance. It was found that the presence of PEG-b-PDCE copolymer affected the morphological structure of the membrane showing its good pore-forming capability. The oil rejection ability and anti-fouling properties of the blend membranes were improved by increasing the PEG-b-PDCE content up to 0.075wt.%. Compared to PVC membrane, the blend membrane prepared with 0.075wt.% PEG-b-PDCE exhibited about four times higher permeability with an excellent oil rejection factor, 98.78%, indicating that the PVC/PEG-b-PDCE blend membranes have high potential in oily wastewater treatment.

Keywords: Ultrafiltration; PVC; PEG-b-PDCE copolymer; Membrane; Oily wastewater.

1. Introduction

High-efficiency and energy-saving technologies have drawn significant consideration in wastewater treatment due to the increased environmental and energy concerns [1,2]. One of the worrisome wastewaters discharged by various petrochemical industries is oily wastewater (OWW) [3]. This contains different hydrocarbons, fats, and petroleum components such as gasoline, diesel, oil, and kerosene [4,5]. Most of oily compounds are found as an oil-in-water emulsion with oil droplet sizes less than 20 μm [6,7]. To move toward the long-waited circular economy and protect the environment, OWW treatment and reuse together with oil recovery are necessary. Traditional separation techniques, including mechanical separation, gravity settling, coagulation, air flotation, and chemical de-emulsification are frequently utilized to treat oil-water emulsions [8–11]. However, these methods have some drawbacks such as high energy consumption, low efficiency, large space requirement, and operational difficulties [11,12]. Instead, membrane-based separation technologies have not only overcome these disadvantages, but are environment-friendly [13–16].

Recently, polyvinyl chloride (PVC) ultrafiltration (UF) membranes have been proposed for the treatment of OWW [17–20]. This was motivated by the low-cost of PVC, its excellent physico-chemical stability, superior mechanical strength, and suitability for membrane formation [21–24]. For instance, PVC is soluble in various solvents like N-methylpyrrolidone (NMP), N,N-dimethylacetamide (DMAc), tetrahydrofuran (THF), dimethylformamide (DMF). In addition, it exhibits high stability in harsh alkaline and acidic environments [25,26]. However, the relatively natural hydrophobic character of PVC membranes induces a high fouling tendency, particularly for OWW feed solutions reducing considerably the membrane permeability and its lifespan while increasing operational costs [27–29].

One of the most popular solutions to membrane fouling issue is to render the membranes more

hydrophilic. In fact, hydrophilic membrane surface often exhibits a higher propensity to generate a hydration layer, which keeps specific foulants away from it [30,31]. In this sense, membrane modification can be carried out by grafting or coating hydrophilic polymers on the membrane surface, incorporating organic/inorganic nano-materials, or by physical blending among others [32–35]. For example, Ahmad *et al*. [36] prepared novel PVC composite UF membranes by blending bentonite and varying the amount of different inorganic salts in the casting solution. An enhanced pure water flux, permeate flux, oil rejection, and fouling resistance ability were obtained for all membranes containing salt and bentonite additives in the casting solution. In another work, Ahmad *et al*. [37] prepared PVC membrane blended with acrylamide grafted bentonite for oily water treatment. The hydrophilic feature (water contact angle 49.1°), pure water flux (293.14 $L.m^{-2}.h^{-1}$), permeate flux (123.96 $L.m^{-2}.h^{-1}$), and oil rejection >93.2%, were enhanced for the modified PVC membrane with bentonite. Although the surface properties are improved by surface coating or surface grafting, and the inner pores are hardly altered, these surface modification methods are post-treatment approaches that increase membrane fabrication steps and costs as consequence [14]. The incorporation of organic/inorganic nano-materials into polymeric membranes must overcome the possible aggregation problem of these nano-additives [20]. The advantages of the blending technique over surface modification and the incorporation of nano-materials are its ability to simultaneously alter the membrane's surface and internal pores without inducing any aggregation issue. [15]. This technique allows the use of a variety of polymeric additives, such as hydrophilic homopolymers or amphiphilic copolymers, endowing the blended membranes exceptional hydrophilicity and anti-fouling performance [3,19,38,39]. However, the weak interactions between hydrophilic homopolymer additives and polymeric membrane matrix reduce the stability of homopolymers during both membrane preparation and usage [6].

Recently, amphiphilic copolymers (i.e. with both hydrophilic and hydrophobic chains), had attracted more attention to improve membrane hydrophilicity as functional blend additives [14,39,40]. The hydrophilic segments of these copolymers can increase membrane hydrophilicity, while the hydrophobic segments serve as anchors being important for the stability of the introduced copolymer in the membrane matrix favoring its compatibility with other membrane polymers as well. Amphiphilic copolymers, both synthetic and commercial, have improved UF membranes' performance in OWW treatment [41–46]. For instance, the commercial Pluronic F127 (PF127) amphiphilic copolymer was considered to improve the oil separation of UF membranes [21,41,42]. PF127 is a tri-block amphiphilic copolymer containing two hydrophilic blocks of polyethylene oxide (PEO) around a center hydrophobic block of polypropylene oxide (PPO). Liu et al. [43] prepared hydrophilic and anti-fouling PVC membranes by adding different quantities of F127 into the casting solution (PVC/Pluronic F127 0-10 wt/wt %). All blended PVC membranes exhibited excellent anti-fouling properties even with the lowest F127 content. The results showed that the PVC blending membrane with 8 wt.% F127 displayed optimized anti-fouling and performance. Ahmad *et al*.[47] prepared PVC-based UF membranes using various salt coagulation baths, NMP solvent, bentonite nanoparticle and PF127 copolymer additives. Among the saturated salt coagulation baths involving NaCl, KCl, NH_4Cl, $MgCl_2$ and $CaCl_2$, the use of the salt KCl coagulation bath resulted in optimally synthesized membranes with a high hydrophilicity character. The optimum composition of the best performed PVC-based membrane involved 14.0, 5.0, 0.7 and 80.3 g of PVC, PF127, bentonite, and NMP, respectively. The permeate flux (i.e., 554.0 $L.m^{-2}.h^{-1}$) as well as the pure water flux (i.e., 1610.0 $L.m^{-2}.h^{-1}$), the percent oil rejection (i.e., 93.4%) and the antifouling properties (i.e., FRR: 75.8%) improved significantly for oil field produced water treatment.

In another research study, Ahmad *et al*. [48] prepared PVC/polyacrylonitrile (PAN)/PF127/bentonite blended UF membranes using a KOH-induced KCl-salt coagulation bath and studied their performance for the purification of oily wastewater. The optimally synthesized membrane was obtained by maximizing the pure water flux. The best performed membrane using 14.0, 1.94, 4.23, 0.66 and 79.17 g of PVC, PAN, PF127, bentonite, and NMP, respectively, exhibited a significant enhancement of the permeate flux, 1760.55 ± 68.2 $L.m^{-2}.h^{-1}$, with oil rejection factors greater than 97.0%. In addition, amphiphilic synthetic copolymers such as di-block copolymers containing poly(ethylene glycol) (PEG) and polystyrene [49], polysulfone-based tri-block copolymers [44], poly(methyl methacrylate)(PMMA)-b-poly(4-vinylpyridine) [45], and PMMA-b-poly(ethylene glycol) methacrylate (PPEGMA) [46] had been used to prepare blend membranes with enhanced anti-fouling characteristics. Rajasekhar et al. [50] synthesized an amphiphilic copolymer containing two polyacrylate-carboxylic acid blocks and one polystyrene block by the reversible addition-fragmentation chain transfer (RAFT) method. The amphiphilic copolymer was mixed with polyvinylidene fluoride (PVDF) to prepare blend membranes by phase inversion technique. The modified membrane displayed 2.5 times greater permeate flux along with an improved molecular weight cut-off (MWCO) compared to the neat PVDF membrane. Liu et al. [51] synthesized PMMA-b-PEG-b-PMMA tri-block copolymer by atom transfer radical polymerization (ATRP) and improved PVDF membrane by blending technique. The results exhibited that the presence of additives in the non-solvent phase inversion (NIPS) technique caused surface segregation, thus the fabricated membrane showed greater fouling resistance during the separation process. Zhao et al. [14] group synthesized combed-shape PEGMA-b-PMMA-b-PPEGMA (PEME) amphiphilic tri-block copolymer by RAFT technique for the preparation of PVDF blended membrane by NIPS method. The results showed a resolved trade-off relationship

between the lower permeate flux and the higher BSA rejection for blend membranes. Roy et al. [3] used a segmented amphiphilic copolymer (PDMS-PEG) of poly(dimethylsiloxane) and poly(ethylene glycol) for the preparation of modified membranes. The results demonstrated the membranes' good anti-fouling properties, a water flux of approximately 280 $L.m^{-2}.h^{-1}$ with oil rejection greater than 99%, and a flux recovery ratio (FRR) as high as 99%.

The use of amphiphilic di-block copolymers for the treatment of OWW is receiving less scientific attention, even though they are more efficient than hydrophilic homopolymers for improving membrane performance. Furthermore, the synthesis of poly(1,2-dichloroethylene) PDCE-based amphiphilic block copolymers for membrane blending has received no attention. In this study, a novel amphiphilic PEG-b-PDCE di-block copolymer was synthesized by means of ATRP technique. This facilitates the preparation of novel copolymers with accurately controlled molecular weight, low dispersity indexes ($M_w/M_n < 1.1$), various functionalities and composition (graft, block, and alternating gradient copolymers) [52,53]. In fact, ATRP polymerization's versatility offers a practical method for designing and preparing modified membranes [54].

By using gel permeation chromatography (GPC) and attenuated total reflection infrared spectroscopy (ATR), the chemical structure of PEG-b-PDCE was examined. Then, by using the NIPS technique, PEG-b-PDCE copolymer was utilized as a modifier to prepare PVC/PEG-b-PDCE blend membranes. The selection of PEG-b-PDCE as a blending modifier is based on the expected surface accumulation affinity of the amphiphilic copolymer owing to the hydrophilic PEG blocks [55]. In addition, PEG is compatible with various membrane host polymers. In this case, the PEG-b-PDCE copolymer, the host polymer PVC and the additive PEG400 form a miscible casting solution. The hydrophobic PDCE and the hydrophilic PEG blocks share structural similarities with PVC and PEG400 polymers, respectively. The ether and ester functional groups

of PEG-b-PDCE allow it to function as a hydrophilic additive. In this study, different analytical methods, including ATR spectra, field emission scanning electron microscopy (FESEM), atomic force microscopy (AFM), differential scanning calorimetry (DSC) and tensile testing were employed for membrane characterization. Furthermore, the contact angle and pure water flux (*PWF*) of the prepared blend membranes were determined, the solute transport technique was used to estimate the pore size and its distribution, and the separation of oil-water emulsions was finally examined.

2. Materials and methods

2.1. Materials

Polyvinyl chloride (PVC, grade E-6834, M_W = 90000) was purchased from Arvand Petrochemical Co., Iran. N,N-dimethylacetamide (DMAc) and sodium dodecyl sulfate ($C_{12}H_{25}NaO_4S$) were supplied from Merck. Anhydrous dichloromethane (DCM), N,N,N′,N″,N″-pentamethyldiethylenetriamine (PMDTA), triethylamine (TEA), polyethylene glycol (PEG) (M_w = 400, 4000, 6000, and 10000 Da), and poly(ethylene glycol) monomethyl ether (mPEG) (M_w = 5000 Da) were purchased from Sigma Aldrich. 2-bromoisobutyryl bromide and copper (I) bromide were supplied from Alfa Aesar. To prepare oil-water emulsion, industrial vegetable oil was utilized.

2.2. Synthesis of macro-initiator mPEG-Br

The macro-initiator (mPEG-Br) was synthesized in terms of the procedure explained by Stubbs et al. [56]. mPEG (Mn ~ 5000, 1 mmol) was first dried using an vacuum oven. The mPEG, TEA (0.56 mL), and anhydrous dichloromethane (20 mL) were combined and cooled to 0 ºC in a

suitable flask under nitrogen atmosphere. Subsequently, 2-bromoisobutyryl bromide (0.49 mL) was added gradually and the reaction was agitated for one night at 25 ºC under nitrogen atmosphere. The agitated solution precipitated into a sizable amount of diethyl ether after being concentrated under a reduced pressure. The precipitate was extracted with dichloromethane after filtration and then dissolved in a saturated sodium bicarbonate solution (20 mL). After being stirred with magnesium sulfate (10 to 20% by weight of solvent) for an hour, the organic layer was filtered. Finally, the product was isolated following the concentration step under a reduced pressure, and then precipitation in diethyl ether. Before usage, the precipitate was dried for 24 h using a vacuum oven.

2.3. Synthesis of mPEG-b-Poly(1, 2-dichloroethylene) di-block copolymer

The mPEG-b-Poly(1, 2-dichloroethylene) di-block copolymer was synthesized using ATRP method as follows. 0.26 mmol macro-initiator mPEG-Br was dissolved in 2 mL tetrahydrofuran (THF) in a suitable flask, and 0.65 mmol 1, 2-dichloroethylene was mixed with 3 mL THF in another flask. Both flasks went through five freezing-pumping-thawing cycles, and 0.30 mmol CuBr and 0.6 mmol PMDTA were introduced in the cycle's last freeze. Before adding the macro-initiator solution into the 1, 2-dichloroethylene solution, two flasks were purged with nitrogen and thawed. The reaction combination was carried out at room temperature (25 ºC) under stirring for 6-12 hours to attain the needed molecular weight. The termination reactions were performed by exposure to air, then diluting it with THF. After filtration through neutral alumina, concentration *in vacuo*, and precipitation in hexane, the copolymer was isolated. Finally, a vacuum oven at 75℃ was used to dry the white solid copolymer PEG-b-Poly(1, 2-dichloroethylene).

2.4. Characterization of the copolymer

The ATR spectra of PEG-b-PDCE were obtained using a VERTEX70 FTIR spectrometer (Bruker, Germany) in the range 400–4000 cm^{-1}. The molecular weights (M_n *and* M_w) and molecular weight distribution (*PDI*) of PEG-b-PDCE were identified on a Viscotek 270 non-aqueous gel permeation chromatography armed with a refractive index detector; 1.0 mL/min THF were utilized as eluent and polystyrene standards were applied in GPC.

2.5. Membrane preparation

Both neat and blended PVC membranes were prepared following NIPS technique. For the blended membrane, a certain amount of PEG-b-PDCE was dispersed in DMAc for at least 30 min; then PEG400 was added into the copolymer solution for pore formation and stirred 10 more minutes. Subsequently, PVC was dissolved in the polymer solution and mixed for at least a full day to produce a homogenous solution. This was then degassed to remove air bubbles. The polymer mixture was cast uniformly on a glass plate at 25 °C. The glass was immediately immersed in a water coagulation bath at 30 ºC for phase separation until the formed polymer layer was simply separated from the surface of the glass plate. The prepared membrane was kept in distilled water for a whole day to take out all residual solvents. Finally, the membranes were dried and kept at 25 ºC before testing. Table. 1 displays the used membrane casting solution's chemical composition.

Table. 1. Chemical composition of the casting solutions used for membrane preparation.

Membranes	PVC (wt.%)	Copolymer (wt.%)	DMAc (wt.%)	PEG400 (wt.%)
M-0	15.0	-	79.000	6.0
M-1	15.0	0.025	78.975	6.0
M-2	15.0	0.050	78.950	6.0
M-3	15.0	0.075	78.925	6.0
M-4	15.0	0.100	78.900	6.0

2.6. Membrane characterization

The chemical composition of the prepared membranes was explored by ATR-FTIR technique using a Tensor 27 FTIR spectrometer (Bruker, Germany) and KBr pellet in the range 400–4000 cm^{-1}. Their thermal properties were studied by a differential scanning calorimetry (DSC 200 F3, Netzsch), following 10 ºC/min heating rate under nitrogen atmosphere. The prepared samples were first equilibrated at 20 ºC and then heated from 20 ºC to 140 ºC at a constant rate of 10 ºC/min, and then cooled back from 140 ºC to -90 ºC. Subsequently, the membrane samples were heated again from -90 ºC to 140 ºC.

The morphological structure of the surface and cross-section of all membranes was considered with a Field Emission Scanning Microscope (FESEM; MIRA3 FEG-SEM, Tescan Co., Czech). First, the membrane samples were broken in liquid nitrogen and then sputtered with a fine gold coating. The elemental mapping of PVC/PEG-b-PDCE blend membrane was verified by EDX (Tescan MIRA3, Japan Czech) to examine the uniform distribution of PEG-b-PDCE throughout the membrane matrix. The top surface roughness of the prepared membranes was determined by AFM (Nanosurf Mobile S, Nanosurf Co., Switzerland). In this case, small membrane samples (1

mm wide and 5 mm long) were prepared, and the AFM analysis was carried out over scanned images of 8 μm × 8 μm area. The hydrophilic character of the membranes was studied by means of the apparent water contact angle measurement [57]. Contact angle of membrane top surface was measured by a contact angle meter (ZAM104-B, Zolalan Co., Iran). Underwater oil contact angle on the membrane surface was measured under water to study the membrane oleophobicity. 3 μL vegetable oil droplet was considered in this case. At least three measurements were taken at different positions on each sample.

The mechanical strength of the prepared membranes was analyzed by a tensile testing device (STM-5, WICK-ROELL, Iran). Their porosity (ε) was measured by the dry-wet technique. The membrane sample was immersed first in water for 24 h. Then, it was removed from water and cleaned gently with a filter paper removing any remaining water droplets. The weights of both the cleaned (i.e. wet) and dried membranes at 60°C were measured. The porosity of each membrane was finally determined using the following equation [58]:

$$\varepsilon\ (\%) = \frac{(W_{wet} - W_{dry})/D_{water}}{(W_{\mathrm{wet}} - W_{dry})/D_{water} + (W_{dry}/D_{polymer})} \times 100 \quad (1)$$

where ε is the bulk porosity of the membrane (%), w_{wet} and w_{dry} are the wet and dry weights of the membrane (g), D_{Water} (0.998) and $D_{Polymer}$ (1.4) in (g/cm^3) are the density of water and PVC, respectively.

Equilibrium water content (*EWC*), which is associated with the porosity, is described as the moisture level where the membrane neither loses nor gains moisture. This was calculated as follows [59]:

$$EWC\ (\%) = \left(\frac{W_{wet} - W_{dry}}{W_{dry}}\right) \times 100 \quad (2)$$

where w_{dry} and w_{wet} are the weight (g) of the dry and wet membrane samples.

More details of the characterization tests can be found elsewhere [18,25].

Molecular weight cut-off (*MWCO*) of membranes is considered as the lowest molecular weight (in Da) at which the membrane retains more than 90% of a solute with a specific molecular weight. The *MWCO* determination is a reliable method for membrane characterization, which is used in membrane processes to describe the pore size estimation and rejection capabilities of membranes. In this study, a water-soluble polymer, polyethylene glycol (0.6, 4, 6, and 10 kDa), was used to prepare aqueous PEG solutions with a concentration of 500 ppm to estimate the *MWCO* of PVC-based membranes. The PEG rejection tests were conducted using PEG solutions at room temperature and 200 kPa operating pressure. First, filtration tests were done by the lab-scale cross-flow system mentioned in section 2.8 and pure water as feed to evaluate pure water fluxes prior PEG rejection experiments. Then, each PEG solution was considered as feed to carry out the solute transport method detailed elsewhere [60,61]. The polymer concentration in the feed ($C_{f,\,PEG}$) and permeate ($C_{p,\,PEG}$) were measured by the refractometer (WAY-2S, Bante, China), and the PEG rejection factor was determined according to the following equation:

$$R_{PEG} = \left(\frac{C_{f,\ PEG} - C_{p,\ PEG}}{C_{f,\ PEG}}\right) \quad (3)$$

The *MWCO*, mean pore size, and the corresponding geometric standard deviation were specified as reported in [60,61]. The PEG rejection factors and the corresponding Einstein-Stokes diameters (Eq. 4) were plotted on a log-normal probability paper. From the obtained straight lines, the *MWCO* and the mean pore size were calculated according to the Einstein-Stokes diameters that correspond to 90% and 50% PEG rejection factors, respectively, while the geometric standard deviation was estimated from the ratio between the Einstein-Stokes diameter corresponding to 84.13% PEG rejection factor and that of 50%.

The Einstein-Stokes diameter of PEG (d_{PEG} in cm) was determined from its molecular weight (M in Da) using the following equation:

$$d_{PEG} = 33.46 \times 10^{-10} M^{0.557} \quad (4)$$

From the mean pore size and the geometric standard deviation values, the pore size distribution can be obtained by the probability density function [60,61]:

$$\frac{\mathrm{d}f(d_p)}{\mathrm{d}(d_p)} = \frac{1}{d_p \ln \sigma_p (2\pi)^{1/2}} \exp\left(-\frac{(\ln d_p - \ln \mu_p)^2}{2(\ln \sigma_p)^2}\right) \quad (5)$$

where d_p, μ_p, and σ_p are the pore size, the mean pore size, and its geometric standard deviation, respectively.

2.7. Preparation of feed oil-water emulsion

The oil in water emulsion was prepared by combining 5 mg/L sodium dodecyl sulfate ($C_{12}H_{25}NaO_4S$) as a surfactant and 1000 mg/L liquid vegetable oil at 2000 rpm for at least 24 h. According to our previous work [20], oil-water emulsion's oil droplet size distribution after 2, 24, and 48 h changed from 0.001 to 48.1 μm, 0.001 to 47.6 μm, and 0.001 to 46.9 μm, respectively; and the average radius of oil droplets was 2.20, 2.11, and 2 μm, respectively. The stability of oil droplets was enhanced with time by introducing SDS in solution [20,62]. Additionally, the maximum oil droplet's size was reported below 20 μm every time, and the oily feed could be considered oil in water emulsion [20,63].

2.8. Filtration experiments

The filtration experiments of the prepared membranes were performed using the lab-scale crossflow system having an active circular membrane area of 28.26 cm^2. A schema of this system is shown in Fig. 1 while the operating conditions are summarized in Table. 2.

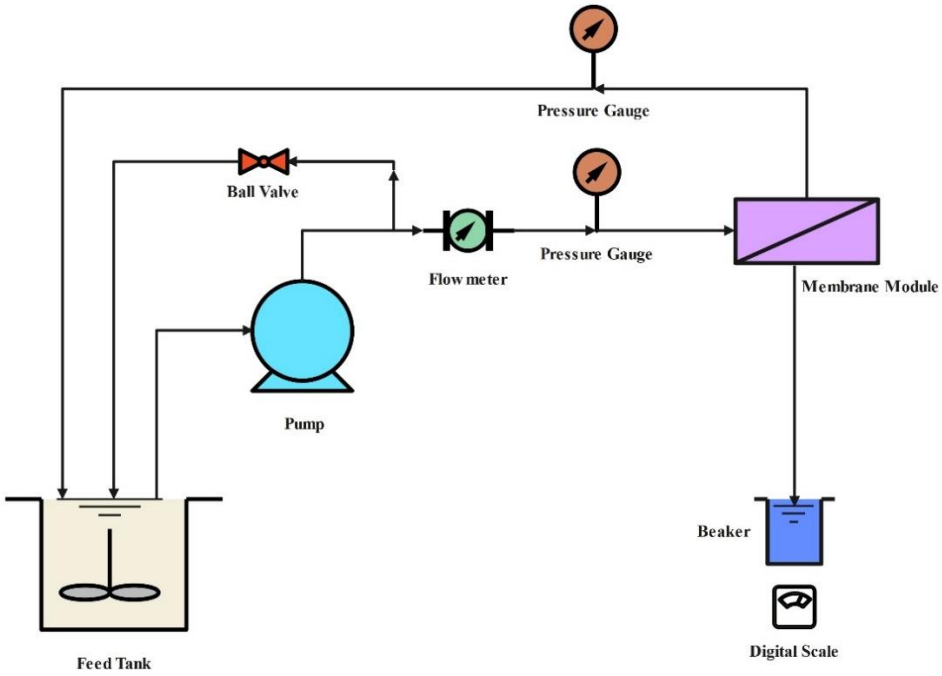

Fig. 1. Schematic diagram of the laboratory-scale crossflow system.

The membrane sample was firstly compacted for 30 min at 2.5 bar and then the pure water flux (J_0) was specified using Eq. (6) [64,65]:

$$J_0 = \frac{V}{A.\Delta t} \quad (6)$$

where V is the volume of pure water (L) registered during the permeation time (Δt in h), and A is the effective membrane area (m^2). The water permeate flux was then divided by the transmembrane hydrostatic pressure to get the pure water permeance of the prepared membranes.

Table. 2. Operational conditions.

Parameter	Value
Pressure (bar)	2.00
Liquid oil concentration (ppm)	1000
Concentration of sodium dodecyl sulfate (ppm)	5.00
Input feed flow rate (L/min)	4.39
pH	6.00
Affective membrane area (cm^2)	28.26

After *PWF* test, the membrane module was connected to feed oily water emulsion tank (1000 mg/L) and the permeate flux was measured for 2.5 h under a transmembrane hydrostatic pressure of 2 bar, applied as driving force through the membrane. To quantify the *PWF* after fouling (*J1*), the membrane module was connected again to the feed water tank for membrane cleaning and *PWF* measurement (J_2). The total fouling ratio (*TFR*), reversible fouling ratio (*RFR*), irreversible fouling ratio (*IFR*), and flux recovery (*FRR*) were computed by means of Eqs. (7)–(10) [66–69] to investigate the fouling behavior of both the neat PVC membrane and the PVC/PEG-b-PDCE blend membranes.

$$TFR = \left(\frac{J_0 - J_1}{J_1}\right) \times 100 \quad (7)$$

$$RFR = \left(\frac{J_0 - J_2}{J_1}\right) \times 100 \quad (8)$$

$$IFR = \left(\frac{J_1 - J_2}{J_1}\right) \times 100 \quad (9)$$

$$FRR = \left(\frac{J_2}{J_1}\right) \times 100 \quad (10)$$

where J_0, J_1 and J_2 was the pure water flux, water flux after fouling, and water flux after washing, respectively. According to the above relationships, it is clear that:

$$TFR = RFR + IFR \quad (11)$$

To study the membrane's ability to remove pollutants from the OWW, the rejection analysis was performed by measuring the turbidity and chemical oxygen demand (COD) in both the feed and treated water. The turbidity of the oily feed and permeate flow were evaluated by turbidity meter (2020We, Lamotte Co., USA). The organic content was measured as total COD in the samples of oily feed and treated water using permanganometric titration. The pollutant rejection was determined using the following equation [70–72]:

$$R_i\ (\%) = \left(\frac{C_{fi} - C_{pi}}{C_{fi}}\right) \times 100 \quad (12)$$

where R_i is the rejection efficiency regarding a specific pollutant, and C_{fi} and C_{pi} are the concentrations of oil in the oily feed and permeate solution, respectively.

3. Results and discussion

3.1. Amphiphilic PEG-b-PDCE di-block copolymer characteristics

The PEG-b-PDCE di-block copolymer, consisting of a hydrophobic PDCE chain segment and a hydrophilic PEG segment was synthesized following the ATRP polymerization procedure. The chemical structure of the used components together with the synthesized amphiphilic copolymer are shown in scheme 1.

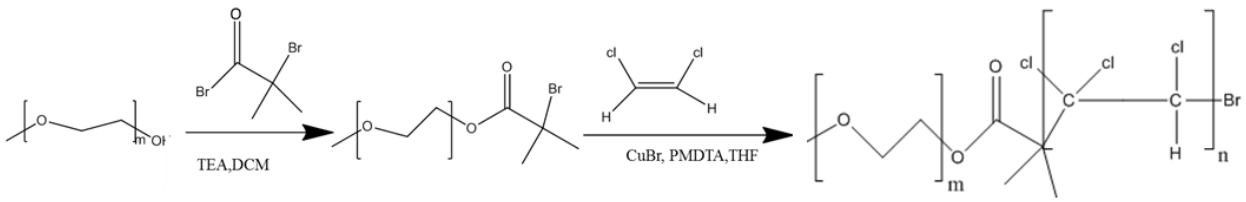

Scheme 1. Preparation of the PEG-b-PDCE di-block copolymer via ATRP polymerization.

The GPC analysis was utilized to assess the molecular weight averages of PEG-b-PDCE s. The obtained molecular weight distribution is depicted in Fig. 2-a. The GPC traces of PEG-b-PDCE exhibited a symmetrical single peak with narrow polydispersity index (*PDI*). The M_n, M_w and *PDI* of the PEG-b-PDCE di-block copolymer were found to be 14252.10 g/mol, 14401.09 g/mol, and 1.01, respectively. As can be seen the *PDI* is quite small and both M_n and M_w values are near each other because the distribution curve is symmetric.

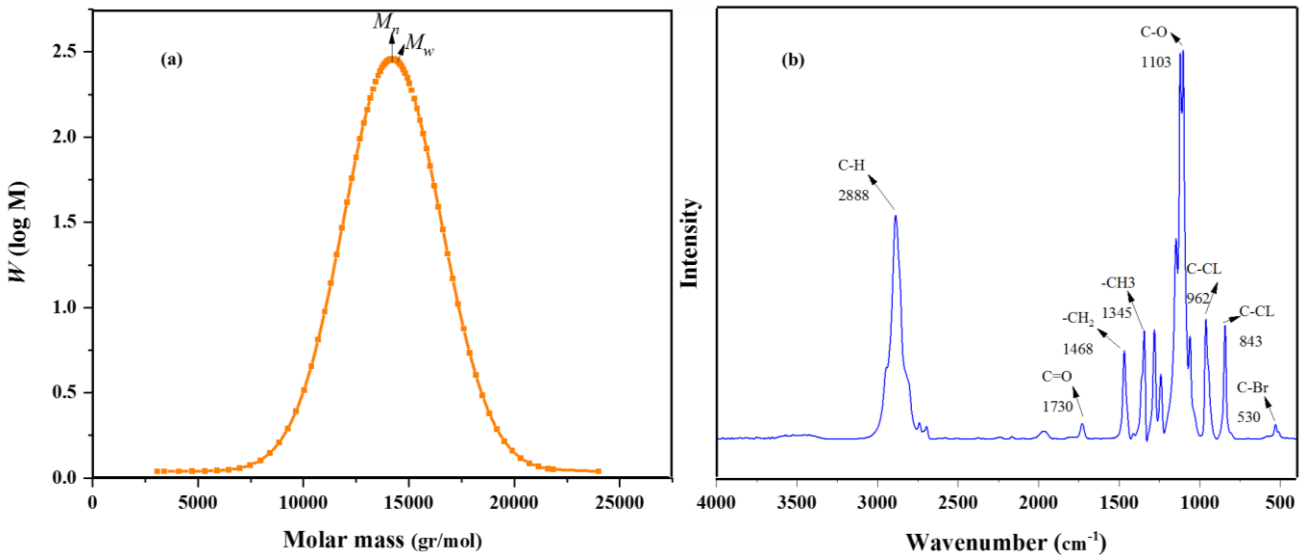

Fig. 2. (a) Molecular weight distribution and (b) ATR spectra of PEG-b-PDCE.

The chemical functional groups of the amphiphilic di-block copolymer PEG-b-PDCE were first analyzed by ATR as shown in Fig. 2-b. In the obtained ATR spectra, the most intense peak at about 1100 cm^{-1} is related to the C−O−C stretching vibration characteristic absorption peak. The observed peak at 1730 cm^{-1} is attributed to the stretching vibration of C=O of PEG-b-PDCE. The appeared typical peaks at 843 cm^{-1} and 962 cm^{-1} are related to the stretching vibration of C−Cl bonds in PEG-b-PDCE most likely due to two different conformations. The results of ATR and GPC indicated that the synthesized PEG-b-PDCE di-block copolymer have been successfully synthesized by ATRP polymerization procedure.

3.2. Effect of the PEG-b-PDCE di-block copolymer on the membrane characteristics

The chemical composition of the membrane surface has an important impact on the hydrophilicity, permeability, and fouling characteristics of the membrane. As depicted in Fig. 3, the ATR spectra of the neat PVC membrane (M-0) and PEG-b-PDCE blended PVC membranes (M-1, M-2, M-3, and M-4) showed absorption bands at about 1400 cm^{-1}, 1250 cm^{-1}, and 900 cm^{-1} due to the CH_2 wagging, skeletal vibration of C−C, and stretching vibration of C−Cl bonds in the

PVC, respectively. The described peaks were intensified by increasing the PEG-b-PDCE blending ratio in the membrane matrix. In contrast to the neat PVC membrane, the ATR spectra of the blended membranes displayed novel peaks at 1732 cm^{-1} associated with the stretching vibration of the ester's carbonyl (C=O) group of the PEG-b-PDCE di-block copolymer. It is important to note that during the NIPS process, PDCE blocks in PEG-b-PDCE operate as anchors because of the interactions between PDCE and PVC matrix, whereas the hydrophilic PEG blocks tend to accumulate on the membrane surface, improving water wettability, permeability, and anti-fouling performance as will be discussed later.

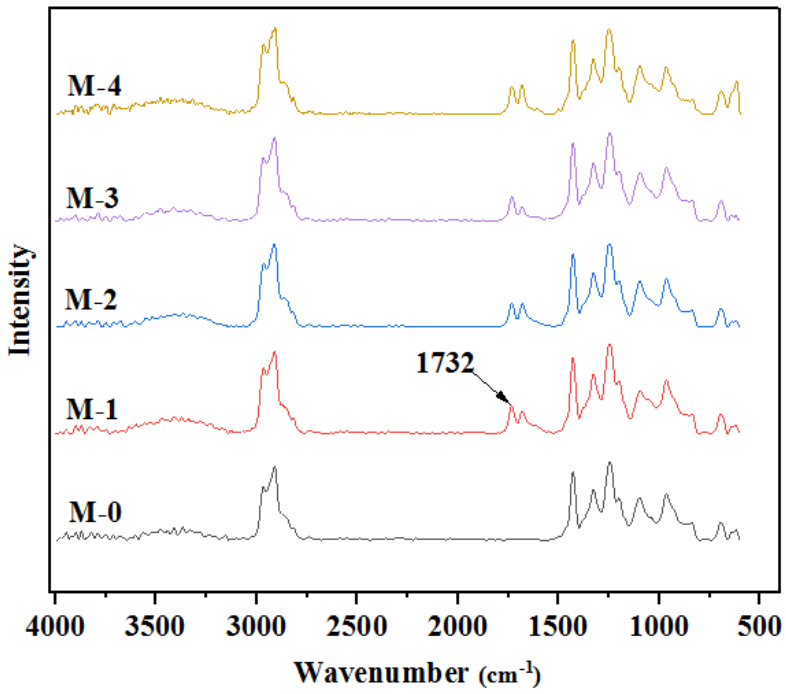

Fig. 3. ATR spectra of the neat PVC and PEG-b-PDCE blended PVC membranes.

To analyze whether the PEG-b-PDCE copolymer was evenly distributed on the surface of the membrane or not, the typical EDX mappings of the C, Cl, and O elements was performed on membrane top surface. The results of the membrane M-3 are presented as an example in Fig. 4. It

was found that C, Cl, and O elements were uniformly distributed on the top surface of the mixed membranes indicating that the hydrophilic PEG chains were dispersed uniformly on the membrane surface.

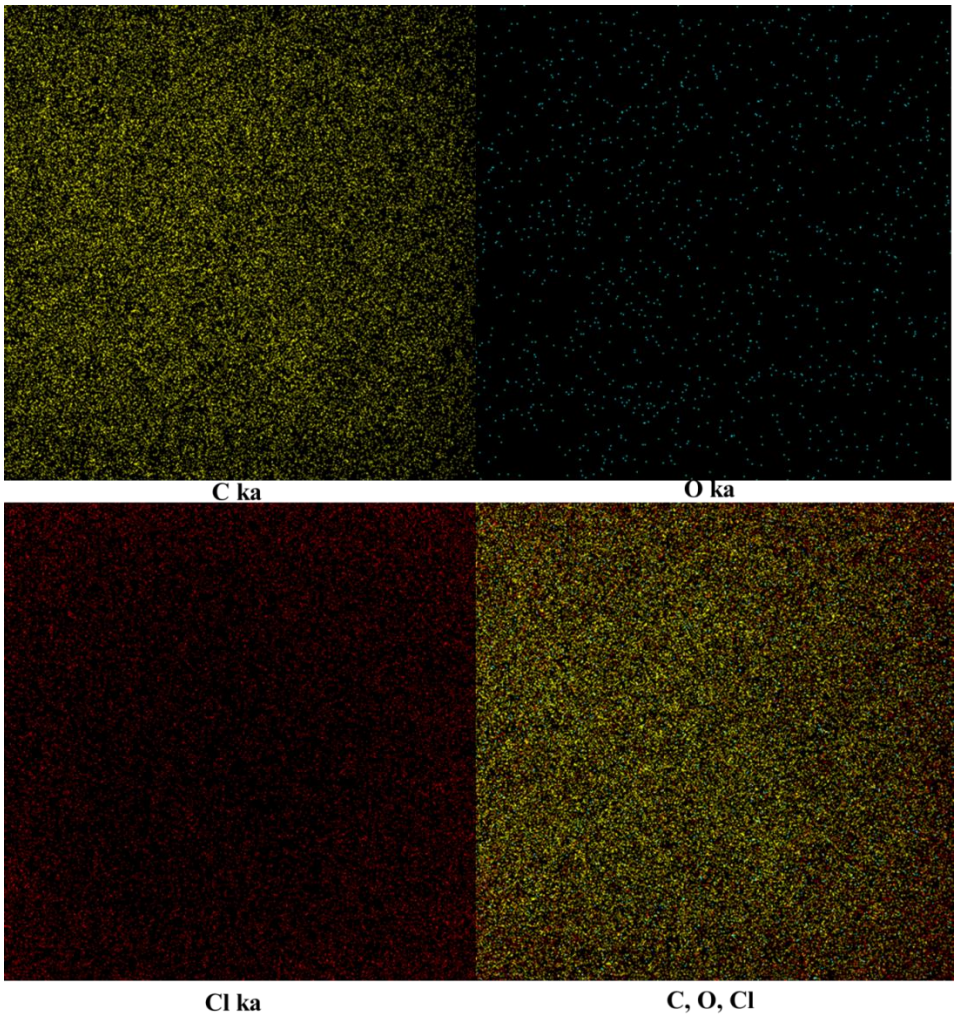

Fig. 4. EDX mappings of the M-3 membrane's top surface for C, O, and Cl elements.

In this study, thermal analysis (DSC) was also carried out to specify the glass transition temperature (T_g) and study the compatibility between PVC and PEG-b-PDCE. The compatibility and interaction between them would clearly influence the structural properties and characteristic of the formed blend membranes [23,73]. It is known that T_g can directly indicate whether two polymers are miscible or not [19,74]. In this case, the DSC analysis was carried out for the

membranes M-0 and M-4 prepared with the highest PEG-b-PDCE copolymer blending content. The DSC curves of the two membranes are plotted in Fig. 5. As it is clear, a single T_g was identified for the M-4 membrane confirming that the PEG-b-PDCE/PVC blend is a mono-phase system resulting in compatible and miscible membranes [29,75].

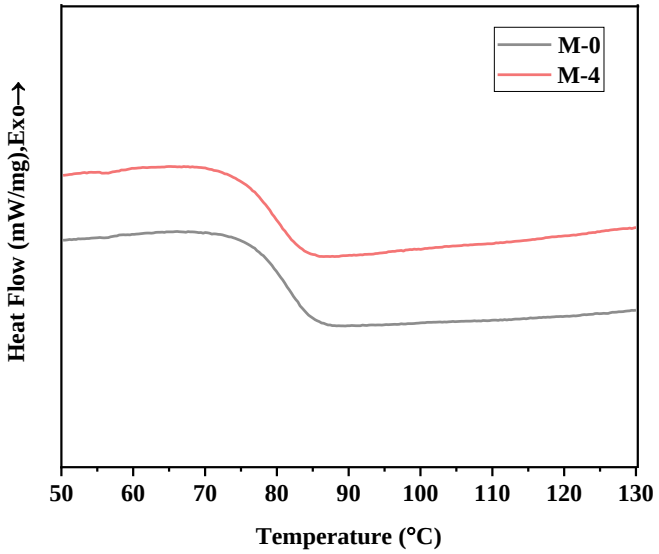

Fig. 5. DSC curves of the membranes M-0 and M-4.

The addition of PEG-b-PDCE di-block copolymer caused only a small change of T_g of the neat PVC membrane (i.e. up on the addition of PEG-b-PDCE, the T_g of the M-0 membrane was decreased from 81.3 ºC to 80.6 ºC for the membrane M-4). It seems that the PEG-b-PDCE copolymer acted as a diluent because it is lower than that of the PVC polymer (i.e. 14401.09 g/mol for PEG-b-PDCE and 90000 g/mol for PVC). Nevertheless, this small reduction of T_g proves the PEG-b-PDCE copolymer is part of the blend membrane matrix.

The effect of the PEG-b-PDCE di-block copolymer on both the cross-section and top surface morphology of the prepared membranes was studied by FESEM as shown in Figs. 6 (a and b). For all prepared membranes, the obtained cross-section images exhibit a common asymmetric

feature consisting of a selective top thin active layer, a finger-like structure layer beneath the skin layer and a macro-voids bottom layer. As it can be seen in Fig. 6-a, compared to the membrane M-0, the PEG-b-PDCE blended PVC membranes exhibited a higher density of finger-like voids with an improved interconnection between them through thicker sponge-like structure. This variation was mostly related to the amphiphilic PEG-b-PDCE copolymer. The relatively hydrophobic PDCE block of the PEG-b-PDCE copolymer would confirm robust anchoring in the PVC matrix owing to their high compatibility, while the hydrophilic PEG block would segregate to water-polymer interface during blend membrane formation by NIPS technique. Zhao et al. group used polyacryloylmorpholine-b-poly (methyl methacrylate)-b-polyacryloylmorpholine triblock amphiphilic copolymers as pore forming additives and improved the hydrophilicity of PVDF membranes [15]. As the casting solution's copolymer content increased from 0.025wt.% (M-1 membrane) to 0.1wt.% (M-4 membrane), longer and interconnected finger-like structure was observed throughout the membrane thickness (Fig. 6(a), M-1 to M-4).

The morphological structure of the top membrane surface is presented in Fig. 6 (b). Changes can be detected between the M-0 membrane and the other PEG-b-PDCE blend membranes. The top surface of the M-0 membrane is relatively denser than that of the blend membranes. This may be attributed to the delayed demixing due to the highly hydrophobic nature of the constituent polymer for the neat PVC membrane compared to the PEG-b-PDCE blend membranes [50]. Rajasekhar et al. reported similar results for neat PVDF and PVDF/amphiphilic tri-block copolymer membranes [50].

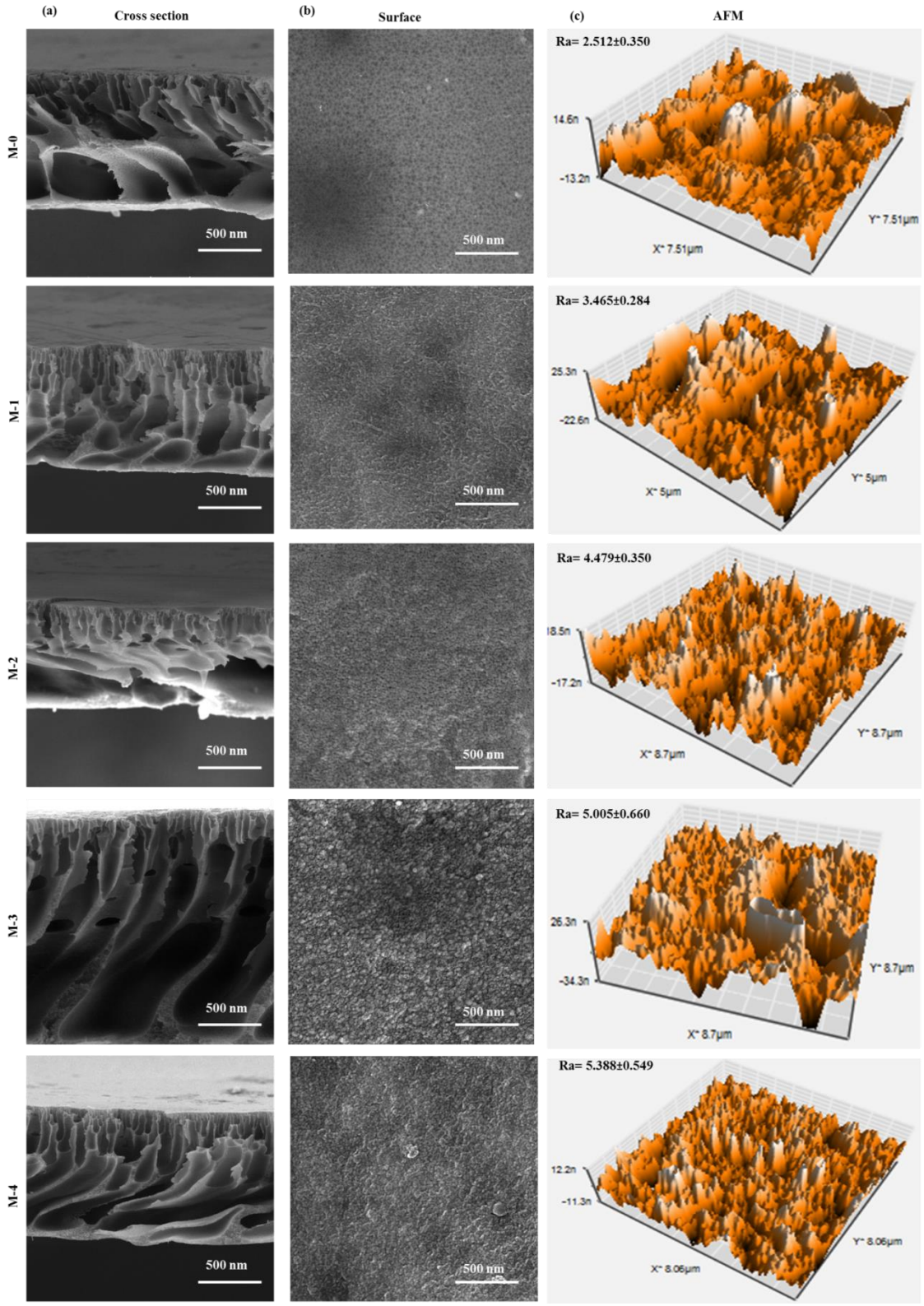

Fig. 6. Cross-section and top surface FESEM and AFM images of the neat PVC membrane and PEG-b-PDCE blended PVC membranes.

The obtained three-dimensional AFM images are also presented in Fig. 6 (c). These also support the FESEM results. In addition, it was observed that the surface mean roughness parameter (*Ra*) is higher for the PEG-b-PDCE blended PVC membranes. Within the scan area of 8 µm × 8 µm, the mean roughness of the M-1, M-2, M-3, and M-4 blend membranes are 3.46±0.28 nm, 4.47±0.35 nm, 5.00±0.66, and 5.38±0.54 nm, respectively. These values are greater than that of the M-0 membrane (*Ra*= 2.512±0.350 nm) confirming that the incorporation of the copolymer not only affected the bulk membrane matrix but also its surface. In fact, the change of the membrane surface roughness may be attributed to the change of nodules and pore sizes as well as the porosity as discussed later on. There are evidences displaying that the addition of amphiphilic copolymers to polymeric membranes renders them rougher [3,14]. According to Zhao et al., the PVDF membrane's roughness increased from 32.1 nm to 147 nm for blend membrane with the addition of 0.9 g polyacryloylmorpholine-b-poly (methyl methacrylate)-b-polyacryloylmorpholine copolymer [15].

The hydrophilic character of the membrane surface is a significant parameter affecting both the permeability and fouling of the membrane during filtration process [57,76,77]. Many substances like oil droplets and biological compounds can quickly accumulate on both the membrane surface and inside its pores during OWW treatment process. An improvement of the membrane surface hydrophilicity can reduce the adsorption of foulants, proteins, or oil droplets on the membrane's surface [28,41]. The measured static water contact angle and underwater oil contact angle of the prepared membranes are displayed in Fig. 7.

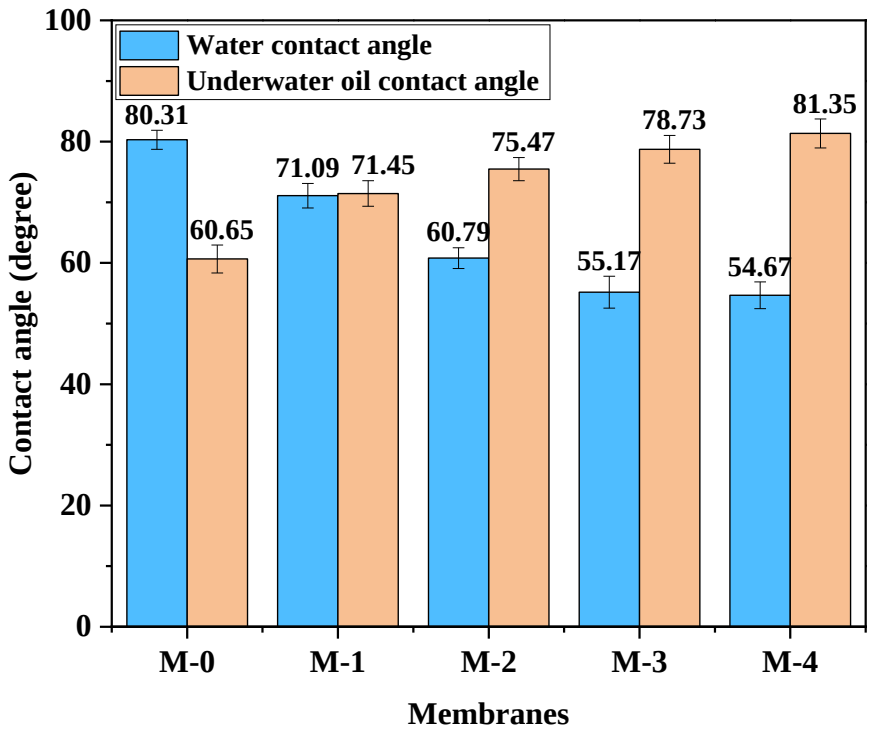

Fig. 7. Static water contact angle and underwater oil contact angle of the neat PVC membrane and PEG-b-PDCE blended PVC membranes.

There is a reduction of the water contact angle upon the rise of the PEG-b-PDCE blending ratio in the PVC membrane. These are 80.31º, 71.09º, 60.79º, 55.17º and 54.67º for the membranes M-0, M-1, M-2, M-3, and M-4, respectively. The pretty high water contact angle for the neat PVC membrane is attributed to the intrinsic relatively hydrophobic nature of the PVC polymer [18,20]. In the literature, contact angles of 80º [78], 88.60º [74,79], 91.80º [80] have been reported for PVC membranes. The gradual increase of the hydrophilic character of the PEG-b-PDCE blended PVC membranes is attributed to the increase of the PEG-b-PDCE blending rate in the PVC casting solution. In other words, this is due to the hydrophilic segment of the PEG-b-PDCE copolymer that segregates at the membrane surface altering therefore the membrane surface properties. The PEG-b-PDCE chains contain reactive functional groups (e.g. ether and ester groups) that boost the interaction with water molecules resulting in an increase of the blend membrane hydrophilicity.

Zhao et al. reported the combination of comb-shaped amphiphilic tri-block copolymer (poly[poly(ethylene glycol) methacrylate]-b-poly (methyl methacrylate)-b-poly[poly(ethylene glycol) methacrylate]) considerably enhanced the hydrophilicity of PVDF membranes [14]. Previous studies reported similar effects of a variety of amphiphilic copolymers [3,50,81]. Based on the obtained underwater oil contact angles, the modified membranes exhibited greater oleophobicity than the neat PVC membrane. Hence, the higher the hydrophilicity in air, the higher the underwater oleophobicity [82].

It must be pointed out that not only the chemical property of the membrane surface is the parameter affecting the measured water contact but also the surface roughness. Based on Wenzel model [41,68], the increase of the surface roughness also improves the wettability brought on by the surface's chemistry. For instance, applying surface roughness effect will make a chemically hydrophobic surface (i.e. with a contact angle greater than 90°) even more hydrophobic, but applying surface roughness effect will increase the hydrophilicity of a hydrophilic material due to the capillary effect [41]. In this case, for PVC membrane surfaces with contact angles less than 90º, surface roughness will reduce the contact angle. As shown earlier, there is an enhancement of the membrane roughness with the increase of the PEG-b-PDCE blending ratio. Therefore, the observed reduction of the water contact with addition of the PEG-b-PDCE copolymer may be related to both the change of the membrane surface chemistry and mean roughness. In addition, it is possible that residual PEG400, used as a pore former, is also contributing to membrane hydrophilicity. Because the interactions between the hydrophilic homopolymer molecules (PEG400) and the hydrophilic blocks of the amphiphilic copolymer (PEG) do not allow them to extract out into water bath in membrane formation. To investigate this possibility, the water contact angle of the prepared membranes was measured after immersion in deionized water for several

493 days. The obtained values are 72.5˚, 62˚, 56˚and 55˚for the M-1, M-2, M-3, and M-4 membranes,
494 respectively. The fact that the water contact angles of the blended membranes were not
495 significantly different indicated that the additive polymers (PEG & PEG-b-PDCE) were stable in
496 the membrane matrix and/or its surface. In addition to the surface chemical heterogeneity, the
497 surface micro/nanostructure is another parameter affecting the underwater oleophobicity. In fact,
498 water molecules can be trapped in rough surfaces and the new composite interface results in an oil
499 repelling property or underwater oleophobicity [82].

500 The measured tensile strength, porosity and *EWC* of the prepared membranes are
501 summarized in Table. 3. The porosity was enhanced from 70.03% to 82.90% as the concentration
502 of the PEG-b-PDCE blending ratio was increased from 0wt.% to 0.075wt.%. A further increase of
503 the PEG-b-PDCE blending ratio to 0.1wt.% (M-4 membrane) resulted in a decline of the porosity
504 by 5.8% compared to that of the M-3 membrane. As discussed previously, this may be related
505 partly to the change of the coagulation speed of blend PVC membrane and to the effect of the
506 amphiphilic PEG-b-PDCE interactions whit PVC and pore former agent.

507 The *EWC* is attributed to the porosity and wettability of the membrane surface. Similar to
508 the porosity, the highest *EWC* (i.e. 79.67%) was obtained for the M-3 membrane. The increase of
509 the *EWC* with the increase of the PEG-b-PDCE blending ratio is due to the rise of water uptake by
510 the PEG-b-PDCE di-block copolymer and the porosity enhancement.

511

512

513

514 Table. 3. *EWC*, porosity, and tensile strength of the neat PVC membrane and PEG-b-PDCE
515 blended PVC membranes.

Membrane	*EWC* (%)	Porosity ε(%)	tensile strength σ (MPa)
M-0	70.83 ± 2.25	70.03 ± 2.66	2.03 ± 0.08
M-1	73.34 ± 1.52	72.13 ± 3.41	1.9 ± 0.05
M-2	75.00 ± 1.00	76.10 ± 2.00	1.84 ± 0.04
M-3	79.67 ± 1.52	82.90 ± 3.08	1.61 ± 0.07
M-4	77.78 ± 1.68	78.33 ± 3.93	1.72 ± 0.09

516

517 Table 3 also shows that the tensile strength of the membranes steadily declined with the
518 increase of the PEG-b-PDCE blending ratio in the casting solution up to 0.075wt.%, and then
519 enhanced for a further increase of the PEG-b-PDCE content. This may be due to the reduction of
520 the porosity (i.e. void volume fraction) of the blend M-4 membrane compared to that of the M-3
521 membrane. These results agree with those reported by Zhao et al. claimed that the mechanical
522 properties of the blended membranes declined as the membrane porosity and pore size were
523 increased [15].

524 As stated earlier, the *MWCO*, mean pore size, and its geometric standard deviation of the
525 prepared membranes were investigated by means of PEG solute transport method. Fig. 8 shows
526 the PEG solute rejection factor as a function of the corresponding PEG Einstein-Stokes diameter
527 on a log-normal probability paper. The experimental data fitted straight lines with relatively high
528 correlation coefficients ($r^2 \geq 0.90$). The different slopes of the obtained lines show the different
529 pore size of the prepared PVC membranes. The results of PEG separation, the *MWCO*, mean pore

size, and the corresponding geometric standard deviation are presented in Table 4. The PEG rejection factor decreased with the increase of the PEG-b-PDCE di-block copolymer content in the casting solution indicating the gradual increase of both the membrane pore size and the *MWCO*. The cumulative pore size distributions and the probability density function curves determined from the mean pore sizes and their geometric standard deviations were plotted in Fig. 9. It can be seen a right-ward shift of the pore size distribution with the increase of the copolymer concentration in the PVC casting solution. However, the observed change was not wide enough since it was only up to 38.4 nm (i.e. maximum pore size of the membrane M-4). Therefore, its effect on the percent oil rejection was negligible. In addition, the increment of the percent oil rejection can be mainly ascribed to the surface heterogeneity and the improved surface hydrophilicity. The detected changes of the *MWCO* and pore size of the PVC membrane are attributed to the addition of the copolymer to the PVC casting solution and to the modification of the phase inversion process as discussed in pervious sections.

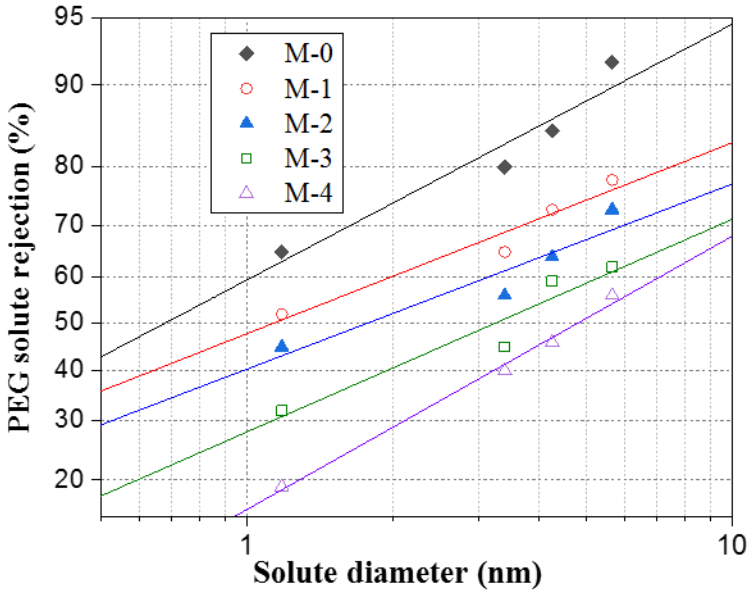

Fig. 8. PEG solute separation curves of the neat PVC membrane and PEG-b-PDCE blended PVC membranes plotted on a log-normal probability paper.

546 Table. 4. PEG solute transport results of the neat PVC membrane and PEG-b-PDCE blended
547 PVC membranes: *MWCO*, mean pore size (μ_p), and geometric standard deviation (σ_p).

Membranes	PEG separation: R_{PEG} (%)				*MWCO* (kDa)	μ_p (nm)	σ_p
	M_W (kDa)						
	0.6	4	6	10			
M-0	65	80	85	92	3.15	1.54	1.76
M-1	52	65	73	78	19.31	3.35	2.14
M-2	45	56	64	73	50.04	5.50	2.20
M-3	32	45	59	62	89.74	8.60	1.98
M-4	19	40	46	56	98.89	10.66	1.73

548

549

550

551

552

553

554

555

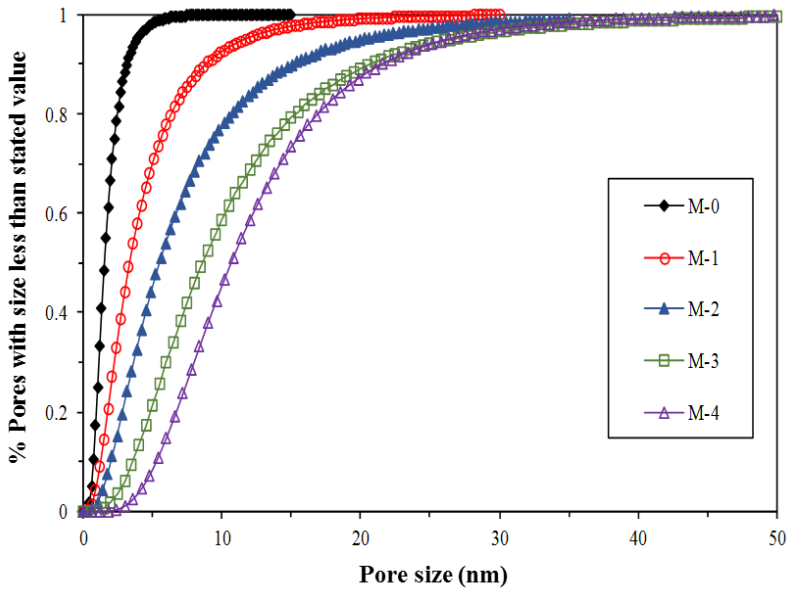

(a)

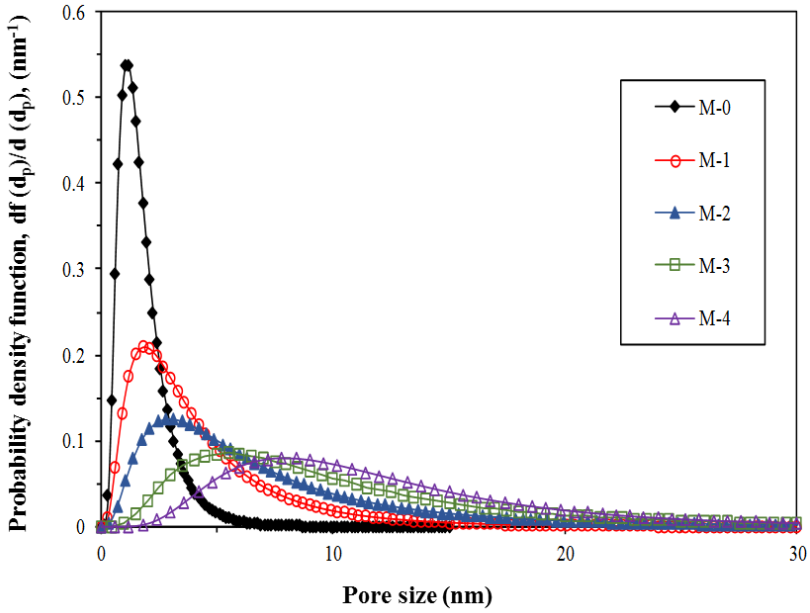

(b)

Fig. 9. Cumulative pore size distributions (a) and probability density function (b) curves of the neat PVC membrane and PEG-b-PDCE blended PVC membranes generated from the PEG solute transport experiments.

3.3. Membrane permeation and separation performance

The membrane morphology and hydrophilicity mostly affect the *PWF* and separation performance. The *PWF* and oil rejection of the neat and PEG-b-PDCE blend membranes were investigated as mentioned in section 2.8. The effect of the PEG-b-PDCE blending ratio on the *PWF* of the prepared PVC membranes are displayed in Fig. 10. It can be observed that the *PWF* raised from 184.03 $L \cdot m^{-2} \cdot h^{-1}$ for the M-0 membrane to a maximum value of 749.11 $L \cdot m^{-2} \cdot h^{-1}$ for the M-3 membrane and then decreased to 629.71 $L \cdot m^{-2} \cdot h^{-1}$ for the M-4 membrane. The observed *PWF* enhancement of the PEG-b-PDCE blend membranes compared to the M-0 membrane is due to the improved hydrophilic character of the blend membranes and the growth of the porosity and pore size with increasing the PEG-b-PDCE blending ratio. Although the M-4 membrane is more hydrophilic than the M-3 membrane, its *PWF* is lower. This is mainly due to the lower porosity of the membrane M-4. Roy et al. [3] also found that the addition of the poly (dimethylsiloxane) and poly(ethylene glycol) amphiphilic co-polymer enhanced the *PWF* of the PVDF/PVP membranes. The permeance of the prepared membranes was also calculated by dividing the *PWF* data by the applied transmembrane hydrostatic pressure (*TMP*). The obtained for the membranes M-0 to M-4 were 92.01, 195.02, 265.39, 374.56, and 314. L.m-2.h-1.bar-1, respectively. Pakbaz *et al*. [83] investigated the performance of PVC/PAN blended UF membrane for the treatment of wastewater and showed that the pure water permeance was limited to only 54.6 $L.m^{-2}.h^{-1}.bar^{-1}$. Pakbaz *et al.* [83] also prepared PVC/PAN/SiO2 and PVC/PAN composite membranes by phase inversion technique using water coagulation bath and a subsequent hydrolysis using aqueous NaOH solution to improve the UF membrane performance. The achieved pure water permeance was 75.6 ± 7.2 $L.m^{-2}.h^{-1}.bar^{-1}$ using hydrolyzed PVC/PAN membrane. Ahmad *et al.* [25] reported that the water permeance for PVC-bentonite blended UF membranes using DMAc as solvent and saturated

aqueous KCl solution as non-solvent was in the range 168.5–183.8 $L.m^{-2}.h^{-1}.bar^{-1}$. Ahmad *et al*. [36] also reported an enhanced pure water flux (i.e., 415.55 $L.m^{-2}.h^{-1}$) for the best performed PVC/bentonite composite membrane. In another study, Ahmad *et al*.[37] obtained an enhanced pure water flux (293.14 $L.m^{-2}.h^{-1}$) for the PVC membrane using acrylamide grafted bentonite. These mentioned results reveal that the PWF of the prepared PEG-b-PDCE blend membranes in this study are higher than the other PVC based membranes.

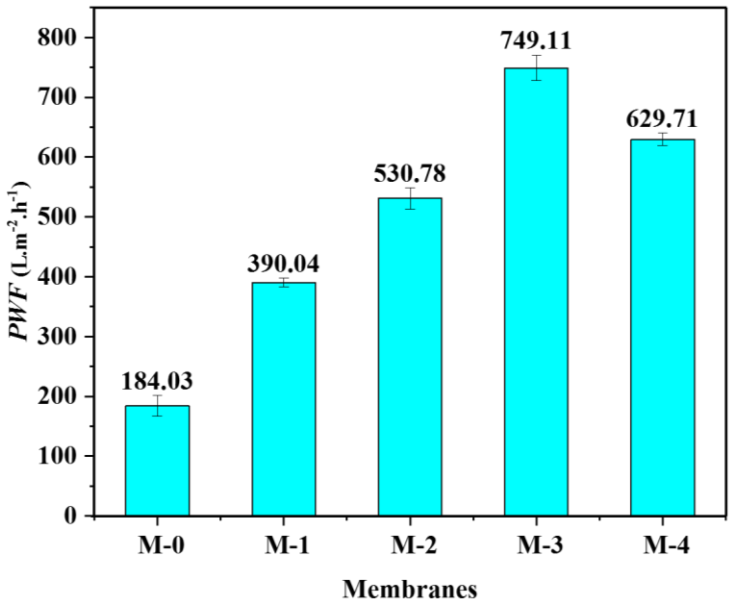

Fig. 10. *PWF* under 2 bar hydrostatic pressure of the neat PVC membrane and PEG-b-PDCE blended PVC membranes.

It is well known that membrane fouling is unavoidable in membrane separation processes resulting in sever decrease of the membrane performance shortening its lifespan [84,85]. The fouling tendency of all prepared membranes was studied using oily wastewater model feed solution as stated in section 2.8. The measured permeate flux is plotted in Fig. 11 against the filtration time.

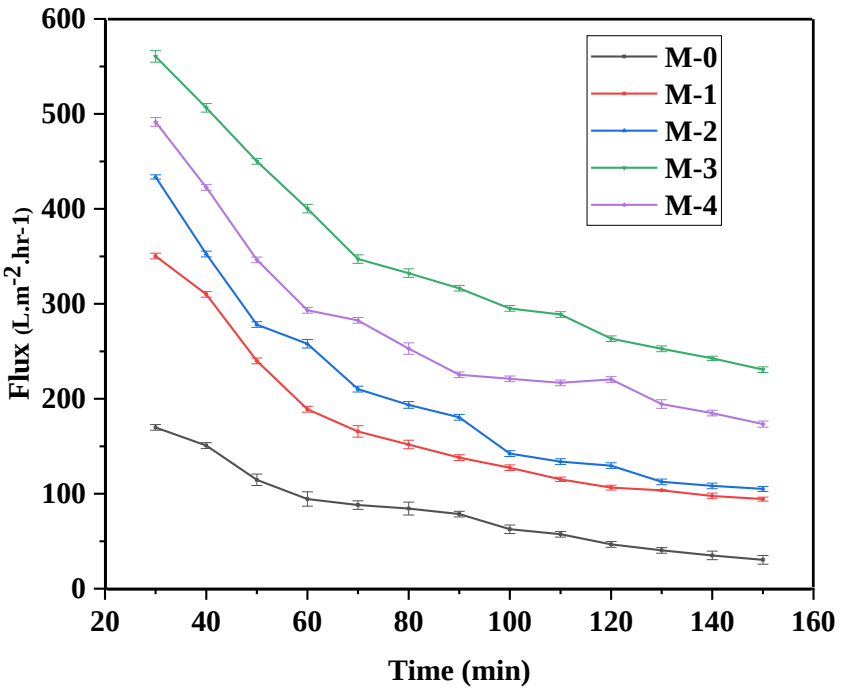

Fig. 11. Permeate flux of the neat PVC membrane and PEG-b-PDCE blended PVC membranes *vs.* filtration time of oily feed wastewater.

All prepared membranes showed a permeate flux decline during the oily feed wastewater treatment. This is due to the deposition of the oily droplets inside the pores and/or on the membrane surface. As observed for distilled water used as feed for filtration (Fig. 10), compared to the PEG-b-PDCE blended PVC membranes, the membrane M-0 had the lowest permeate flux, and after 150 min, its permeate flux decreased 82.3%, from 169 $L \cdot m^{-2} \cdot h^{-1}$ to about 30 $L \cdot m^{-2} \cdot h^{-1}$. However, the permeate flux decline of the neat PVC membrane was higher than that of the PEG-b-PDCE blend PVC membranes, 73%, 75%, 58%, and 64% for the membranes M-1, M-2, M-3, and M-4, respectively. This indicated that the blend membranes exhibited stronger fouling resistance than the M-0 membrane. This is related to the more hydrophilic character of the blend PVC membrane surface as discussed previously in relation with the PEG chains of the di-block copolymer that are hydrophilic. Another factor related that may have contributed to this result is the pore structure

and size may also exert some effects. It was found that membranes with bigger surface pores are more likely to be blocked or fouled by oily drops than those with smaller pores [74,86]. However, in the present study, although the surface pore size of the PVC membranes increased up on the addition of the PEG-b-PDCE copolymer and its concentration in the PVC casting solution, the hydrophilic PEG chains enriched on the blend membrane surface seemed to play a significant role since these chains interact easily with water molecules to create a hydration layer avoiding the interaction of oily foulants with membrane surface.

The determined fouling factors (*TFR*, *RFR*, *IFR*, and *FR*) defined in section 2.8 are shown in Fig. 12. Both reversible and irreversible fouling take place during membrane separation [87], due to either poor or strong interactions between foulant(s) and membrane surface, respectively. In irreversible fouling, the tougher bonding of foulants to membrane surface necessitates chemical treatment, which could harm the membrane and reduce its lifespan. As can be observed in Fig. 12, the M-0 membrane exhibited the maximum *TFR* and *IFR* factors indicating that it was fouled simply by oil droplets. This happens due to the strong affinity between the oil drops and the M-0 membrane matrix. As it is clear in Fig. 12, the *TFR* factor of the membranes declined from 92.58% for the M-0 membrane to 70.97% for the M-3 membrane but it increased again for the M-4 membrane. However, the level of *TFR* and *IFR* factors for all blend membranes was lower than that of the membrane M-0. A lower value of *TFR* shows an improved anti-fouling properties. Accordingly, the *TFR* results showed that the PEG-b-PDCE blend PVC membranes were less likely to foul than the neat PVC membrane, and the M-3 membrane exhibited the lowest fouling tendency in oily wastewater separation. As seen in Fig. 12, by increasing the PEG-b-PDCE blending ratio, *RFR*, *FR*, and the reversible fouling ratio (*RFR/TFR*) increased to a maximum value for the membrane M-3 and then decreased for the membrane M-4. Additionally, compared to the

M-0 membrane, all blend PVC membranes displayed higher reversible fouling tendency and permeate flux recovery. In fact, the PEG-b-PDCE blend membranes had better anti-fouling property owing to their improved hydrophilicity. As a result, the M-3 membrane possessed an excellent anti-fouling behavior due to its surface hydrophilicity and suitable pore structure. Therefore, it can be stated that the addition of the PEG-b-PDCE copolymer into the polymer matrix could reduce the fouling tendency of PVC membranes by reducing the adsorption of oily compounds by the blend membrane surface because the PEG chains of the PEG-b-PDCE copolymer created a strong hydration coating on the membrane surface.

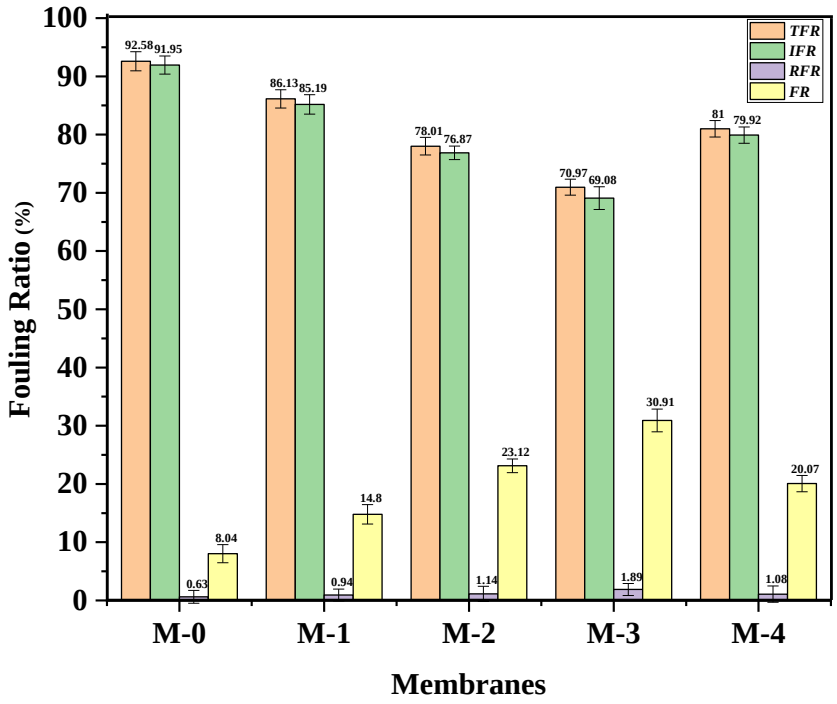

Fig. 12. Fouling ratio (*TFR*, *RFR*, *IFR*, and *FR*) of the neat PVC membrane and PEG-b-PDCE blended PVC membranes.

The rejection efficiency of the PEG-b-PDCE blend PVC membranes was studied by measuring the turbidity and COD parameters of both the feed and permeate during oil-water separation. It is well known that the nature of the amphiphilic polymer ingredients dictates the

affinity between the membrane material and the contaminant elements. As a consequence, the difference in affinity and size exclusion play vital roles in determining the separation efficiency. In this case, the turbidity removal and COD efficiency can reflect these important roles. The measured turbidity and COD parameters of both permeate and feed oily wastewater are summarized in Table 5. The rejection factor with regards to oil pollutant and organic dissolved compounds evaluated by Eq. (12), are presented Fig.13 for all prepared membranes in this study.

Table. 5. Measured turbidity and COD at the end of the ultrafiltration for the permeate and feed oily wastewater of the neat PVC membrane and PEG-b-PDCE blended PVC membranes.

Feed and permeate	Turbidity (NTU)	COD (mg/L)
Feed	35.00	362.63
Permeate (M-0)	3.34	127.95
Permeate (M-1)	2.50	105.75
Permeate (M-2)	1.85	74.00
Permeate (M-3)	1.78	51.38
Permeate (M-4)	2.10	67.69

The turbidity and COD values of the permeate were much lower that of the feed oily wastewater indicating pretty high rejection efficiency of micro-sized oily particles (i.e. the rejection factor based on turbidity were greater than 97.5 % for all blend membranes while that based on COD were higher than 70.8%). The rejection factors of the M-0 membrane (90.5% based on turbidity and 64.7% based on COD, respectively) were lower than those of the PEG-b-PDCE blended PVC membranes. For all membranes, the observed higher rejection factor based on

turbidity than that based on COD may be due to the substances to be separated by the membranes. Pollutants that require chemical oxidation can be soluble and/or insoluble in water, while the turbidity of the synthetic wastewater is caused by undissolved oil droplets. Therefore, the membranes were able to reject well oily droplets but perform less in rejecting organic compounds. These observations agree with the separation mechanism and potential of ultrafiltration (UF) membranes, particularly the sieving mechanism [14].

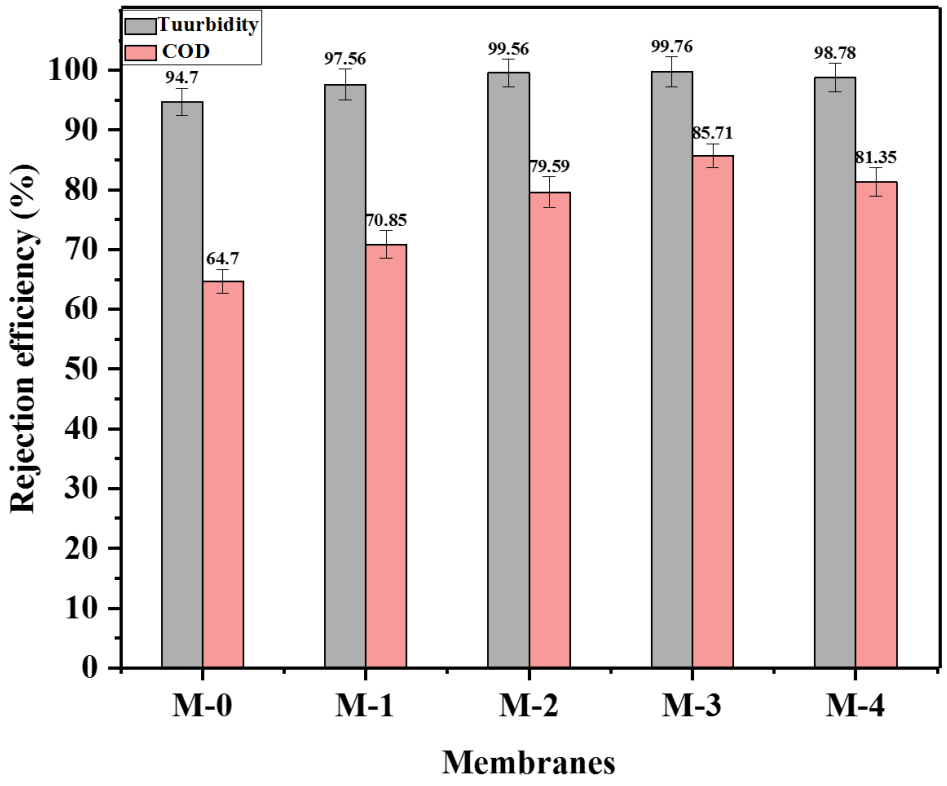

Fig.13. Rejection factors based on turbidity and COD of the neat PVC membrane and the PEG-b-PDCE blend PVC membranes.

According to the given data in Table 5 and Fig. 13, the rejection factors improved with the increase of the PEG-b-PDCE blending ratio in the casting solution up to 0.075wt.% and then dropped for 0.1wt.% (i.e. membrane M-4). The M-3 membrane exhibited the highest rejection

factors because of its hydrophilic surface and suitable pore structure. The enrichment of the hydrophilic PEG chains of the PEG-b-PDCE di-block copolymer on the membrane surface renders it prone to mix with water molecules and form a hydrated layer avoiding therefore oil molecules to be in contact with the membrane surface and resulting in a good oil rejection factor as consequence.

4. Conclusions

PEG-b-PDCE amphiphilic di-block copolymer was synthesized by ATRP procedure and proposed as additive for PVC blend membrane preparation by NIPS technique. The prepared membranes were proposed for oil-water emulsion separation. The appearance of C=O bonding in ATR spectra of the PEG-b-PDCE blend PVC membranes confirmed the successful introduction of the copolymer in PVC matrix. A single T_g was observed in DSC curve for all blend membranes indicating the good compatibility of PVC and PEG-b-PDCE di-block copolymer. The chemical and morphological characteristics of the PVC membrane were changed with the PEG-b-PDCE blending ratio in the casting solution. The PEG-b-PDCE blend membranes exhibited rougher surfaces and higher density of finger-like voids with an improved interconnection. The increase of the PEG-b-PDCE blending ratio in the casting solution from 0wt.% to 0.075wt.% increased the porosity, *EWC*, and surface roughness up to a maximum and then decreased for 0.1wt.%. As a result, both the permeation and rejection factors of the PEG-b-PDCE blend PVC membranes were greater than those of the neat PVC membrane because of their improved characteristic such as higher contact angle, interconnected finger-like pores, greater pore size and higher porosity. The PEG-b-PDCE di-block copolymer enhanced the anti-fouling resistance of the PVC membrane. Among all prepared membranes, the M-3 membrane containing only 0.075wt.% PEG-b-PDCE

blending ratio was found to be the best one exhibiting 749.11 $L.m^{-2}.h^{-1}$ permeate flux, 99.71% oil rejection factor, 85.71% rejection factor based on COD, and 70.97% total fouling ratio due to its higher surface hydrophilicity and higher porosity. In general, the PEG-b-PDCE di-block blend copolymer proved to be a good candidate for PVC membrane engineering and can be tested for other host polymers and other separation applications.

References

[1] J. Zhao, G. He, G. Liu, F. Pan, H. Wu, W. Jin, Z. Jiang, Manipulation of interactions at membrane interfaces for energy and environmental applications, Prog. Polym. Sci. 80 (2018) 125–152. https://doi.org/10.1016/j.progpolymsci.2017.12.002.

[2] J.R. Werber, C.O. Osuji, M. Elimelech, Materials for next-generation desalination and water purification membranes, Nat. Rev. Mater. 1 (2016) 1–15. https://doi.org/10.1038/natrevmats.2016.18.

[3] S. Roy, D. V. Bhalani, S.K. Jewrajka, Surface segregation of segmented amphiphilic copolymer of poly(dimethylsiloxane) and poly(ethylene glycol) on poly(vinylidene fluoride) blend membrane for oil–water emulsion separation, Sep. Purif. Technol. 232 (2020) 115940. https://doi.org/10.1016/j.seppur.2019.115940.

[4] S. Jamaly, A. Giwa, S.W. Hasan, Recent improvements in oily wastewater treatment: Progress, challenges, and future opportunities, J. Environ. Sci. 37 (2015) 15–30. https://doi.org/10.1016/J.JES.2015.04.011.

[5] C.P.M. de Oliveira, M.M. Viana, G.R. Silva, L.S. Frade Lima, E. Coutinho de Paula, M.C.S. Amaral, Potential use of green TiO2 and recycled membrane in a photocatalytic membrane reactor for oil refinery wastewater polishing, J. Clean. Prod. 257 (2020) 120526.

https://doi.org/10.1016/J.JCLEPRO.2020.120526.

[6] T. Ahmad, C. Guria, A. Mandal, A review of oily wastewater treatment using ultrafiltration membrane : A parametric study to enhance the membrane performance, J. Water Process Eng. 36 (2020) 101289. https://doi.org/10.1016/j.jwpe.2020.101289.

[7] A. Fakhru'l-Razi, A. Pendashteh, L.C. Abdullah, D.R.A. Biak, S.S. Madaeni, Z.Z. Abidin, Review of technologies for oil and gas produced water treatment, J. Hazard. Mater. 170 (2009) 530–551. https://doi.org/10.1016/J.JHAZMAT.2009.05.044.

[8] C.L. Yang, Electrochemical coagulation for oily water demulsification, Sep. Purif. Technol. 54 (2007) 388–395. https://doi.org/10.1016/j.seppur.2006.10.019.

[9] S. Qiu, B. Jiang, X. Zheng, J. Zheng, C. Zhu, M. Wu, Hydrophobic and fire-resistant carbon monolith from melamine sponge: A recyclable sorbent for oil-water separation, Carbon N. Y. 84 (2015) 551–559. https://doi.org/10.1016/j.carbon.2014.12.055.

[10] L. WU, G. GE, J. WAN, Biodegradation of oil wastewater by free and immobilized Yarrowia lipolytica W29, J. Environ. Sci. 21 (2009) 237–242. https://doi.org/10.1016/S1001-0742(08)62257-3.

[11] J.A. Prince, S. Bhuvana, V. Anbharasi, N. Ayyanar, K.V.K. Boodhoo, G. Singh, Ultra-wetting graphene-based PES ultrafiltration membrane – A novel approach for successful oil-water separation, Water Res. 103 (2016) 311–318. https://doi.org/10.1016/J.WATRES.2016.07.042.

[12] J.A. Prince, S. Bhuvana, V. Anbharasi, N. Ayyanar, K.V.K. Boodhoo, G. Singh, Ultra-wetting graphene-based PES ultrafiltration membrane – A novel approach for successful oil-water separation, Water Res. 103 (2016) 311–318. https://doi.org/10.1016/J.WATRES.2016.07.042.

771 [13] A. El-abbassi, H. Kiai, A. Hafidi, M.C. García-payo, M. Khayet, Treatment of olive mill
772 wastewater by membrane distillation using polytetrafluoroethylene membranes, Sep. Purif.
773 Technol. 98 (2012) 55–61. https://doi.org/10.1016/j.seppur.2012.06.026.
774 [14] J. Zhao, Q. Wang, J. Yang, Y. Li, Z. Liu, L. Zhang, Y. Zhao, S. Zhang, L. Chen, Comb-
775 shaped amphiphilic triblock copolymers blend PVDF membranes overcome the
776 permeability-selectivity trade-off for protein separation, Sep. Purif. Technol. 239 (2020)
777 116596. https://doi.org/10.1016/j.seppur.2020.116596.
778 [15] J. Zhao, H. Han, Q. Wang, C. Yan, D. Li, J. Yang, X. Feng, N. Yang, Y. Zhao, L. Chen,
779 Hydrophilic and anti-fouling PVDF blend ultrafiltration membranes using
780 polyacryloylmorpholine-based triblock copolymers as amphiphilic modifiers, React. Funct.
781 Polym. 139 (2019) 92–101. https://doi.org/10.1016/j.reactfunctpolym.2019.03.018.
782 [16] A. Hussain, M. Al-Yaari, Development of polymeric membranes for oil/water separation,
783 Membranes (Basel). 11 (2021) 1–15. https://doi.org/10.3390/membranes11010042.
784 [17] T. Ahmad, C. Guria, Progress in the modification of polyvinyl chloride (PVC) membranes:
785 A performance review for wastewater treatment, J. Water Process Eng. 45 (2022) 102466.
786 https://doi.org/10.1016/j.jwpe.2021.102466.
787 [18] T. Ahmad, C. Guria, A. Mandal, Synthesis, characterization and performance studies of
788 mixed-matrix poly(vinyl chloride)-bentonite ultrafiltration membrane for the treatment of
789 saline oily wastewater, Process Saf. Environ. Prot. 116 (2018) 703–717.
790 https://doi.org/10.1016/j.psep.2018.03.033.
791 [19] Y.X. Xie, K.K. Wang, W.H. Yu, M.B. Cui, Y.J. Shen, X.Y. Wang, L.F. Fang, B.K. Zhu,
792 Improved permeability and antifouling properties of polyvinyl chloride ultrafiltration
793 membrane via blending sulfonated polysulfone, J. Colloid Interface Sci. 579 (2020) 562–

572. https://doi.org/10.1016/j.jcis.2020.06.097.

[20] F. Kazemi, Y. Jafarzadeh, S. Masoumi, M. Rostamizadeh, Oil-in-water emulsion separation by PVC membranes embedded with GO-ZnO nanoparticles, J. Environ. Chem. Eng. 9 (2021) 104992. https://doi.org/10.1016/j.jece.2020.104992.

[21] T. Ahmad, C. Guria, A. Mandal, Kinetic modeling and simulation of non-solvent induced phase separation: Immersion precipitation of PVC-based casting solution in a finite salt coagulation bath, Polymer (Guildf). 199 (2020) 122527. https://doi.org/10.1016/j.polymer.2020.122527.

[22] S. Mei, C. Xiao, X. Hu, Preparation of porous PVC membrane via a phase inversion method from PVC/DMAc/water/additives, J. Appl. Polym. Sci. 120 (2011) 557–562. https://doi.org/10.1002/app.33219.

[23] Y. Cui, Z.K. Yao, K. Zheng, S.Y. Du, B.K. Zhu, L.P. Zhu, C.H. Du, Positively-charged nanofiltration membrane formed by quaternization and cross-linking of blend PVC/P(DMA-co-MMA) precursors, J. Memb. Sci. 492 (2015) 187–196. https://doi.org/10.1016/j.memsci.2015.05.019.

[24] X. Fan, Y. Su, X. Zhao, Y. Li, R. Zhang, J. Zhao, Z. Jiang, J. Zhu, Y. Ma, Y. Liu, Fabrication of polyvinyl chloride ultrafiltration membranes with stable antifouling property by exploring the pore formation and surface modification capabilities of polyvinyl formal, J. Memb. Sci. 464 (2014) 100–109. https://doi.org/10.1016/j.memsci.2014.04.005.

[25] T. Ahmad, C. Guria, A. Mandal, Optimal synthesis and operation of low-cost polyvinyl chloride/bentonite ultrafiltration membranes for the purification of oilfield produced water, J. Memb. Sci. 564 (2018) 859–877. https://doi.org/10.1016/j.memsci.2018.07.093.

[26] D. Ghazanfari, D. Bastani, S.A. Mousavi, Preparation and characterization of poly (vinyl

817 chloride) (PVC) based membrane for wastewater treatment, J. Water Process Eng. 16 (2017)
818 98–107. https://doi.org/10.1016/J.JWPE.2016.12.001.
819 [27] C. Wu, Z. Wang, S. Liu, Z. Xie, H. Chen, X. Lu, Simultaneous permeability, selectivity and
820 antibacterial property improvement of PVC ultrafiltration membranes via in-situ
821 quaternization, J. Memb. Sci. 548 (2018) 50–58.
822 https://doi.org/10.1016/J.MEMSCI.2017.11.008.
823 [28] S.Y. Wang, L.F. Fang, L. Cheng, S. Jeon, N. Kato, H. Matsuyama, Novel ultrafiltration
824 membranes with excellent antifouling properties and chlorine resistance using a poly(vinyl
825 chloride)-based copolymer, J. Memb. Sci. 549 (2018) 101–110.
826 https://doi.org/10.1016/j.memsci.2017.11.074.
827 [29] M. Yong, Y. Zhang, S. Sun, W. Liu, Properties of polyvinyl chloride (PVC) ultrafiltration
828 membrane improved by lignin: Hydrophilicity and antifouling, J. Memb. Sci. 575 (2019)
829 50–59. https://doi.org/10.1016/J.MEMSCI.2019.01.005.
830 [30] A.L. Ahmad, U.R. Farooqui, N.A. Hamid, Effect of graphene oxide (GO) on
831 Poly(vinylidene fluoride-hexafluoropropylene) (PVDF- HFP) polymer electrolyte
832 membrane, Polymer (Guildf). 142 (2018) 330–336.
833 https://doi.org/10.1016/J.POLYMER.2018.03.052.
834 [31] X. Lü, X. Wang, L. Guo, Q. Zhang, X. Guo, L. Li, Preparation of PU modified PVDF
835 antifouling membrane and its hydrophilic performance, J. Memb. Sci. 520 (2016) 933–940.
836 https://doi.org/10.1016/J.MEMSCI.2016.08.018.
837 [32] S.Y. Wang, L.F. Fang, L. Cheng, S. Jeon, N. Kato, H. Matsuyama, Improved antifouling
838 properties of membranes by simple introduction of zwitterionic copolymers via electrostatic
839 adsorption, J. Memb. Sci. 564 (2018) 672–681.

https://doi.org/10.1016/J.MEMSCI.2018.07.076.

[33] L. Zhu, H. Song, D. Zhang, G. Wang, Z. Zeng, Q. Xue, Negatively charged polysulfone membranes with hydrophilicity and antifouling properties based on in situ cross-linked polymerization, J. Colloid Interface Sci. 498 (2017) 136–143. https://doi.org/10.1016/J.JCIS.2017.03.055.

[34] M.A. Tofighy, T. Mohammadi, M.H. Sadeghi, High-flux PVDF/PVP nanocomposite ultrafiltration membrane incorporated with graphene oxide nanoribbones with improved antifouling properties, J. Appl. Polym. Sci. 138 (2021) 1–15. https://doi.org/10.1002/app.49718.

[35] T.D. Kusworo, N. Aryanti, F. Dalanta, Effects of incorporating ZnO on characteristic, performance, and antifouling potential of PSf membrane for PRW treatment, IOP Conf. Ser. Mater. Sci. Eng. 1053 (2021) 012134. https://doi.org/10.1088/1757-899x/1053/1/012134.

[36] T. Ahmad, C. Guria, S. Shekhar, Effects of inorganic salts in the casting solution on morphology of poly(vinyl chloride)/bentonite ultrafiltration membranes, Mater. Chem. Phys. 280 (2022) 125805. https://doi.org/10.1016/J.MATCHEMPHYS.2022.125805.

[37] T. Ahmad, X. Liu, C. Guria, Preparation of polyvinyl chloride (PVC) membrane blended with acrylamide grafted bentonite for oily water treatment, Chemosphere. 310 (2023) 136840. https://doi.org/10.1016/J.CHEMOSPHERE.2022.136840.

[38] T. Tavangar, F. Zokaee Ashtiani, M. Karimi, Morphological and performance evaluation of highly sulfonated polyethersulfone/polyethersulfone membrane for oil/water separation, J. Polym. Res. 27 (2020). https://doi.org/10.1007/s10965-020-02202-5.

[39] L. guang Wu, L. lu Huang, Y. Yao, Z. hao Liu, T. Wang, X. yang Yang, C. ying Dong, Fabrication of polyvinylidene fluoride blending membrane coupling with microemulsion

polymerization and their anti-fouling performance, Polymer (Guildf). 203 (2020) 122767. https://doi.org/10.1016/j.polymer.2020.122767.

[40] Y. Liu, Y. Su, Y. Li, X. Zhao, Z. Jiang, Improved antifouling property of PVDF membranes by incorporating an amphiphilic block-like copolymer for oil/water emulsion separation, RSC Adv. 5 (2015) 21349–21359. https://doi.org/10.1039/c4ra16290k.

[41] Y. Zhang, X. Tong, B. Zhang, C. Zhang, H. Zhang, Y. Chen, Enhanced permeation and antifouling performance of polyvinyl chloride (PVC) blend Pluronic F127 ultrafiltration membrane by using salt coagulation bath (SCB), J. Memb. Sci. 548 (2018) 32–41. https://doi.org/10.1016/j.memsci.2017.11.003.

[42] J.S.B. Melbiah, D. Nithya, D. Mohan, Surface modification of polyacrylonitrile ultrafiltration membranes using amphiphilic Pluronic F127/CaCO3 nanoparticles for oil/water emulsion separation, Colloids Surfaces A Physicochem. Eng. Asp. 516 (2017) 147–160. https://doi.org/10.1016/j.colsurfa.2016.12.008.

[43] B. Liu, C. Chen, W. Zhang, J. Crittenden, Y. Chen, Low-cost antifouling PVC ultrafiltration membrane fabrication with Pluronic F 127: Effect of additives on properties and performance, Desalination. 307 (2012) 26–33. https://doi.org/10.1016/J.DESAL.2012.07.036.

[44] Y.F. Zhao, L.P. Zhu, Z. Yi, B.K. Zhu, Y.Y. Xu, Improving the hydrophilicity and fouling-resistance of polysulfone ultrafiltration membranes via surface zwitterionicalization mediated by polysulfone-based triblock copolymer additive, J. Memb. Sci. 440 (2013) 40–47. https://doi.org/10.1016/J.MEMSCI.2013.03.064.

[45] J. Zeng, C. Lv, G. Liu, Z. Zhang, Z. Dong, J.Y. Liu, Y. Wang, A novel ion-imprinted membrane induced by amphiphilic block copolymer for selective separation of Pt(IV) from

aqueous solutions, J. Memb. Sci. 572 (2019) 428–441. https://doi.org/10.1016/j.memsci.2018.11.016.

[46] J. Meyer, M. Ulbricht, Poly(ethylene oxide)-block-poly(methyl methacrylate) diblock copolymers as functional additive for poly(vinylidene fluoride) ultrafiltration membranes with tailored separation performance, J. Memb. Sci. 545 (2018) 301–311. https://doi.org/10.1016/j.memsci.2017.09.034.

[47] T. Ahmad, C. Guria, A. Mandal, Optimal synthesis, characterization and antifouling performance of Pluronic F127/bentonite-based super-hydrophilic polyvinyl chloride ultrafiltration membrane for enhanced oilfield produced water treatment, J. Ind. Eng. Chem. 90 (2020) 58–75. https://doi.org/10.1016/j.jiec.2020.06.023.

[48] T. Ahmad, C. Guria, A. Mandal, Optimal synthesis of high fouling-resistant PVC-based ultrafiltration membranes with tunable surface pore size distribution and ultralow water contact angle for the treatment of oily wastewater, Sep. Purif. Technol. 257 (2021) 117829. https://doi.org/10.1016/j.seppur.2020.117829.

[49] A. Venault, J.R. Wu, Y. Chang, P. Aimar, Fabricating hemocompatible bi-continuous PEGylated PVDF membranes via vapor-induced phase inversion, J. Memb. Sci. 470 (2014) 18–29. https://doi.org/10.1016/j.memsci.2014.07.014.

[50] T. Rajasekhar, M. Trinadh, P. Veera Babu, A.V.S. Sainath, A.V.R. Reddy, Oil-water emulsion separation using ultrafiltration membranes based on novel blends of poly(vinylidene fluoride) and amphiphilic tri-block copolymer containing carboxylic acid functional group, J. Memb. Sci. 481 (2015) 82–93. https://doi.org/10.1016/j.memsci.2015.01.030.

[51] D. Liu, D. Li, D. Du, X. Zhao, A. Qin, X. Li, C. He, Antifouling PVDF membrane with

909 hydrophilic surface of terry pile-like structure, J. Memb. Sci. 493 (2015) 243–251.
910 https://doi.org/10.1016/j.memsci.2015.07.005.
911 [52] V. Coessens, T. Pintauer, K. Matyjaszewski, Functional polymers by atom transfer radical
912 polymerization, Prog. Polym. Sci. 26 (2001) 337–377. https://doi.org/10.1016/S0079-
913 6700(01)00003-X.
914 [53] K. Matyjaszewski, Atom Transfer Radical Polymerization (ATRP): Current status and
915 future perspectives, Macromolecules. 45 (2012) 4015–4039.
916 https://doi.org/10.1021/MA3001719/ASSET/IMAGES/MEDIUM/MA-2012-
917 001719_0030.GIF.
918 [54] J. Ran, L. Wu, Z. Zhang, T. Xu, Atom transfer radical polymerization (ATRP): A versatile
919 and forceful tool for functional membranes, Prog. Polym. Sci. 39 (2014) 124–144.
920 https://doi.org/10.1016/J.PROGPOLYMSCI.2013.09.001.
921 [55] J.F. Hester, P. Banerjee, A.M. Mayes, Preparation of Protein-Resistant Surfaces on
922 Poly(vinylidene fluoride) Membranes via Surface Segregation, Macromolecules. 32 (1999)
923 1643–1650. https://doi.org/10.1021/MA980707U.
924 [56] E. Stubbs, E. Laskowski, P. Conor, D.A. Heinze, D. Karis, E.M. Glogowski, Control of pH-
925 and temperature-responsive behavior of mPEG-b-PDMAEMA copolymers through
926 polymer composition, J. Macromol. Sci. Part A Pure Appl. Chem. 54 (2017) 228–235.
927 https://doi.org/10.1080/10601325.2017.1282694.
928 [57] M. Khayet, Membrane surface modification and characterization by X-ray photoelectron
929 spectroscopy, atomic force microscopy and contact angle measurements, Appl. Surf. Sci.
930 238 (2004) 269–272. https://doi.org/10.1016/j.apsusc.2004.05.259.
931 [58] C.J. Sajitha, D. Mohan, Studies on cellulose acetate-carboxylated polysulfone blend

ultrafiltration membranes. III, J. Appl. Polym. Sci. 97 (2005) 976–988. https://doi.org/10.1002/app.21799.

[59] O.. A. and M.. D. M.S Rameetse, Synthesis and characterization of PSF / PES composite membranes for use in oily wastewater treatment Synthesis and characterization of PSF / PES composite membranes for use in oily wastewater treatment, (2019). https://doi.org/10.1088/1742-6596/1378/2/022013.

[60] M. Khayet, C.Y. Feng, K.C. Khulbe, T. Matsuura, Preparation and characterization of polyvinylidene fluoride hollow fiber membranes for ultrafiltration, Polymer (Guildf). 43 (2002) 3879–3890. https://doi.org/10.1016/S0032-3861(02)00237-9.

[61] M. Khayet, T. Matsuura, Determination of surface and bulk pore sizes of flat-sheet and hollow-fiber membranes by atomic force microscopy, gas permeation and solute transport methods, Desalination. 158 (2003) 57–64. https://doi.org/10.1016/S0011-9164(03)00433-8.

[62] Y. Yang, A. Raza, F. Banat, K. Wang, The separation of oil in water (O/W) emulsions using polyether sulfone & nitrocellulose microfiltration membranes, J. Water Process Eng. 25 (2018) 113–117. https://doi.org/10.1016/J.JWPE.2018.07.007.

[63] S. Zarghami, T. Mohammadi, M. Sadrzadeh, Preparation, characterization and fouling analysis of in-air hydrophilic/underwater oleophobic bio-inspired polydopamine coated PES membranes for oily wastewater treatment, J. Memb. Sci. 582 (2019) 402–413. https://doi.org/10.1016/J.MEMSCI.2019.04.020.

[64] M.N.A. Seman, M. Khayet, N. Hilal, Comparison of two different UV-grafted nanofiltration membranes prepared for reduction of humic acid fouling using acrylic acid and N-vinylpyrrolidone, Desalination. 287 (2012) 19–29.

955 https://doi.org/10.1016/j.desal.2010.10.031.
956 [65] L.F. Fang, B.K. Zhu, L.P. Zhu, H. Matsuyama, S. Zhao, Structures and antifouling
957 properties of polyvinyl chloride/poly(methyl methacrylate)-graft-poly(ethylene glycol)
958 blend membranes formed in different coagulation media, J. Memb. Sci. 524 (2017) 235–
959 244. https://doi.org/10.1016/j.memsci.2016.11.026.
960 [66] Y. Jafarzadeh, R. Yegani, Analysis of fouling mechanisms in TiO2 embedded high density
961 polyethylene membranes for collagen separation, Chem. Eng. Res. Des. 93 (2015) 684–695.
962 https://doi.org/10.1016/J.CHERD.2014.06.001.
963 [67] M. Javadi, Y. Jafarzadeh, R. Yegani, S. Kazemi, PVDF membranes embedded with PVP
964 functionalized nanodiamond for pharmaceutical wastewater treatment, Chem. Eng. Res.
965 Des. 140 (2018) 241–250. https://doi.org/10.1016/j.cherd.2018.10.029.
966 [68] Y. Jafarzadeh, R. Yegani, M. Sedaghat, Preparation, characterization and fouling analysis
967 of ZnO/polyethylene hybrid membranes for collagen separation, Chem. Eng. Res. Des. 94
968 (2015) 417–427. https://doi.org/10.1016/j.cherd.2014.08.017.
969 [69] F. Beygmohammdi, H. Nourizadeh Kazerouni, Y. Jafarzadeh, H. Hazrati, R. Yegani,
970 Preparation and characterization of PVDF/PVP-GO membranes to be used in MBR system,
971 Chem. Eng. Res. Des. 154 (2020) 232–240. https://doi.org/10.1016/J.CHERD.2019.12.016.
972 [70] M. Khayet, J.I. Mengual, Effect of salt concentration during the treatment of humic acid
973 solutions by membrane distillation, 168 (2004) 373–381.
974 [71] R. Bentini, A. Pola, L.G. Rizzi, A. Athanassiou, D. Fragouli, A highly porous solvent free
975 PVDF/expanded graphite foam for oil/water separation, Chem. Eng. J. 372 (2019) 1174–
976 1182. https://doi.org/10.1016/j.cej.2019.04.196.
977 [72] T.D. Kusworo, N. Ariyanti, D.P. Utomo, Effect of nano-TiO2 loading in polysulfone

membranes on the removal of pollutant following natural-rubber wastewater treatment, J. Water Process Eng. 35 (2020) 101190. https://doi.org/10.1016/j.jwpe.2020.101190.

[73] L.F. Fang, S. Jeon, Y. Kakihana, J. ichi Kakehi, B.K. Zhu, H. Matsuyama, S. Zhao, Improved antifouling properties of polyvinyl chloride blend membranes by novel phosphate based-zwitterionic polymer additive, J. Memb. Sci. 528 (2017) 326–335. https://doi.org/10.1016/J.MEMSCI.2017.01.044.

[74] A. Behboudi, Y. Jafarzadeh, R. Yegani, Polyvinyl chloride/polycarbonate blend ultrafiltration membranes for water treatment, J. Memb. Sci. 534 (2017) 18–24. https://doi.org/10.1016/j.memsci.2017.04.011.

[75] J. Liu, Y. Su, J. Peng, X. Zhao, Y. Zhang, Y. Dong, Z. Jiang, Preparation and Performance of Antifouling PVC/CPVC Blend Ultrafiltration Membranes, Ind. Eng. Chem. Res. 51 (2012) 8308–8314. https://doi.org/10.1021/IE300878F.

[76] E. Demirel, B. Zhang, M. Papakyriakou, S. Xia, Y. Chen, Fe2O3 nanocomposite PVC membrane with enhanced properties and separation performance, J. Memb. Sci. 529 (2017) 170–184. https://doi.org/10.1016/j.memsci.2017.01.051.

[77] A. Pagidi, R. Saranya, G. Arthanareeswaran, A.F. Ismail, T. Matsuura, Enhanced oil-water separation using polysulfone membranes modified with polymeric additives, Desalination. 344 (2014) 280–288. https://doi.org/10.1016/j.desal.2014.03.033.

[78] A. Omidvar, S. Masoumi, M. Monsefi, Y. Jafarzadeh, M. Nasiri, H. Hazrati, PVC/PMMA blend ultrafiltration membranes for oil-in-water emulsion separation, Polym. Bull. 80 (2022) 9275–9295. https://doi.org/10.1007/s00289-022-04514-6.

[79] S. Masoumi Khosroshahi, A. Miroliaei, Y. Jafarzadeh, Preparation and characterization of MWCNT-COOH/PVC ultrafiltration membranes to use in water treatment, Adv. Environ.

Technol. 4 (2018) 95–105. https://doi.org/10.22104/aet.2018.2965.1144.

[80] S. Khakpour, Y. Jafarzadeh, R. Yegani, Incorporation of graphene oxide/nanodiamond nanocomposite into PVC ultrafiltration membranes, Chem. Eng. Res. Des. 152 (2019) 60–70. https://doi.org/10.1016/j.cherd.2019.09.029.

[81] F.C. Guangfa Zhang, Fan Gao, Qinghua Zhang, Xiaoli Zhan, Enhanced oil-fouling resistance of poly(ether sulfone) membrane by incorporating novel amphiphilic zwitterionic copolymers, J. Mater. Chem. C. 3 (2015) 10715–10722. https://doi.org/10.1039/b000000x.

[82] S. Zarghami, T. Mohammadi, M. Sadrzadeh, B. Van der Bruggen, Superhydrophilic and underwater superoleophobic membranes - A review of synthesis methods, Prog. Polym. Sci. 98 (2019) 101166. https://doi.org/10.1016/j.progpolymsci.2019.101166.

[83] M. Pakbaz, Z. Maghsoud, Performance evaluation of polyvinylchloride/polyacrylonitrile ultrafiltration blend membrane, Iran. Polym. J. (English Ed. 26 (2017) 833–849. https://doi.org/10.1007/s13726-017-0568-3.

[84] M. Laqbaqbi, J.A. Sanmartino, M. Khayet, C. Garc, applied sciences Fouling in Membrane Distillation , Osmotic Distillation and Osmotic Membrane Distillation, Appl. Sci. 7 (2017) 334. https://doi.org/10.3390/app7040334.

[85] B. Jiang, B. Hu, N. Yang, L. Zhang, Y. Sun, X. Xiao, G. Di Bella, O. Savadogo, membranes Study of Turbulence Promoters in Prolonging Membrane Life, (2021). https://doi.org/10.3390/membranes11040268.

[86] X. Fu, T. Maruyama, T. Sotani, H. Matsuyama, Effect of surface morphology on membrane fouling by humic acid with the use of cellulose acetate butyrate hollow fiber membranes, J. Memb. Sci. 320 (2008) 483–491. https://doi.org/10.1016/j.memsci.2008.04.027.

[87] L. Zhang, Z. Zhu, U. Azhar, J. Ma, Y. Zhang, C. Zong, S. Zhang, Synthesis of Well-Defined

PVDF-Based Amphiphilic Block Copolymer via Iodine Transfer Polymerization for Antifouling Membrane Application, Ind. Eng. Chem. Res. 57 (2018) 8689–8697. https://doi.org/10.1021/ACS.IECR.8B00533/SUPPL_FILE/IE8B00533_SI_001.PDF.